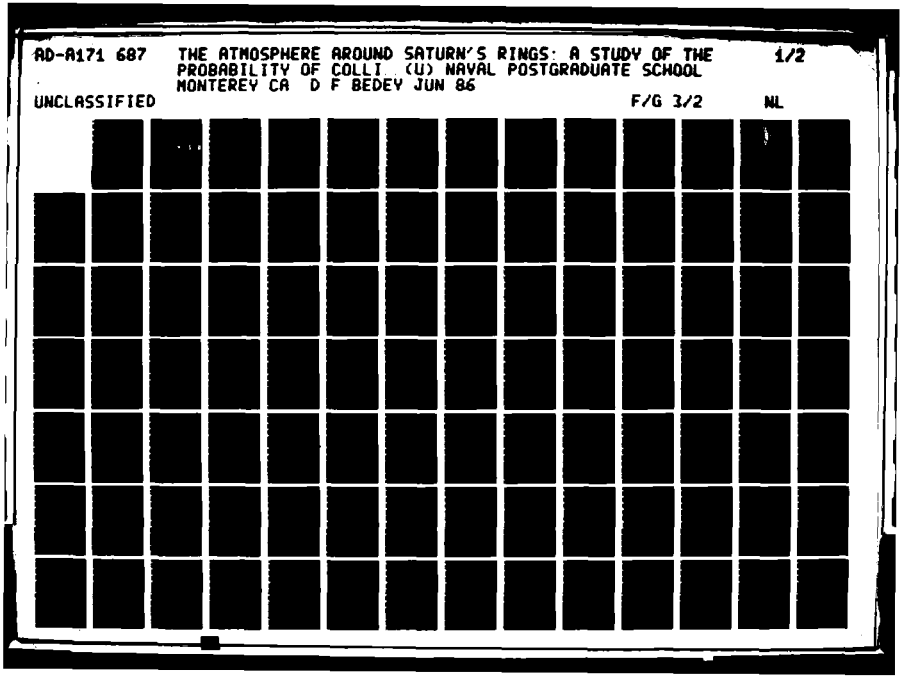
AD-A171 687
THE ATMOSPHERE AROUND SATURN'S RINGS: A STUDY OF THE PROBABILITY OF COLLI (U) NAVAL POSTGRADUATE SCHOOL MONTEREY CA D F BEDEY JUN 86
1/2
UNCLASSIFIED
F/G 3/2
NL

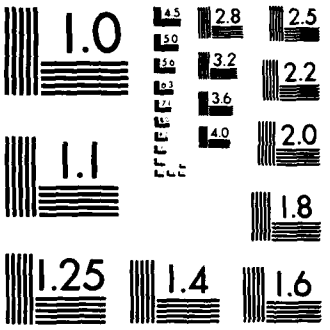

NAVAL POSTGRADUATE SCHOOL
Monterey, California

THESIS

THE ATMOSPHERE AROUND SATURN'S RINGS:
A STUDY OF THE PROBABILITY OF COLLISION
BETWEEN RING PARTICLES AND ATMOSPHERIC
MOLECULES

by

David Franklin Bedey

June 1986

Thesis Advisor: Robert L. Armstead

Approved for public release; distribution is unlimited

UNCLASSIFIED
SECURITY CLASSIFICATION OF THIS PAGE

AD-A171 689

REPORT DOCUMENTATION PAGE

1a REPORT SECURITY CLASSIFICATION UNCLASSIFIED	1b. RESTRICTIVE MARKINGS
2a SECURITY CLASSIFICATION AUTHORITY	3 DISTRIBUTION / AVAILABILITY OF REPORT Approved for public release; distribution is unlimited
2b DECLASSIFICATION / DOWNGRADING SCHEDULE	
4 PERFORMING ORGANIZATION REPORT NUMBER(S)	5 MONITORING ORGANIZATION REPORT NUMBER(S)
6a. NAME OF PERFORMING ORGANIZATION Naval Postgraduate School 6b. OFFICE SYMBOL (If applicable) Code 61	7a. NAME OF MONITORING ORGANIZATION Naval Postgraduate School
6c. ADDRESS (City, State, and ZIP Code) Monterey, California 93943-5000	7b. ADDRESS (City, State, and ZIP Code) Monterey, California 93943-5000
8a NAME OF FUNDING / SPONSORING ORGANIZATION 8b. OFFICE SYMBOL (If applicable)	9. PROCUREMENT INSTRUMENT IDENTIFICATION NUMBER
8c. ADDRESS (City, State, and ZIP Code)	10 SOURCE OF FUNDING NUMBERS PROGRAM ELEMENT NO / PROJECT NO / TASK NO / WORK UNIT ACCESSION NO

11 TITLE (Include Security Classification)
THE ATMOSPHERE AROUND SATURN'S RINGS: A STUDY OF THE PROBABILITY OF COLLISION BETWEEN RING PARTICLES AND ATMOSPHERIC MOLECULES

12 PERSONAL AUTHOR(S)
Bedey, David F.

13a TYPE OF REPORT	13b TIME COVERED	14 DATE OF REPORT (Year, Month, Day)	15 PAGE COUNT
Master's Thesis	FROM _____ TO _____	1986, June	101

16 SUPPLEMENTARY NOTATION

17 COSATI CODES			18. SUBJECT TERMS (Continue on reverse if necessary and identify by block number)
FIELD	GROUP	SUB-GROUP	Ring Atmosphere; Saturn; Collision Probability

19 ABSTRACT (Continue on reverse if necessary and identify by block number)

An analytic model is developed to allow derivation of the probability that a molecule in the atmosphere of Saturn's rings collides with at least one ring particle when traversing the ring plane. The resulting expression involves details of the molecule's trajectory, including the velocity of the molecule relative to ring particles; thus, the theory is compatible with recently developed ballistic-transport computer models used in the analysis of the rings. The collision theory is applied to the case of a low energy, isotropic molecular production process to make inferences on the spatial extent of the ring atmosphere associated with such a source. The high frequency of collisions expected for the atmosphere in the vicinity of the A and B rings suggests a toroidal atmosphere.

20 DISTRIBUTION / AVAILABILITY OF ABSTRACT ☒ UNCLASSIFIED/UNLIMITED ☐ SAME AS RPT ☐ OTIC USERS	21 ABSTRACT SECURITY CLASSIFICATION Unclassified
22a NAME OF RESPONSIBLE INDIVIDUAL Robert L. Armstead	22b TELEPHONE (Include Area Code) (408) 646-2125 22c OFFICE SYMBOL Code 61Ar

DD FORM 1473, 84 MAR 83 APR edition may be used until exhausted
All other editions are obsolete

SECURITY CLASSIFICATION OF THIS PAGE
UNCLASSIFIED

Approved for public release; distribution is unlimited

The Atmosphere Around Saturn's Rings: A Study of the Probability of Collision Between Ring Particles and Atmospheric Molecules

by

David Franklin Bedey
Captain, United States Army
B.S., Montana State University, 1977

Submitted in partial fulfillment of the requirements for the degree of

MASTER OF SCIENCE IN PHYSICS

from the

NAVAL POSTGRADUATE SCHOOL
June 1986

Author: David F Bedey
David Franklin Bedey

Approved by:
Robert L. Armstead, Thesis Advisor

K E Woehler
Karlheinz E. Woehler, Second Reader

William B. Colson
Gordon E. Schacher, Chairman,
Department of Physics

John N. Dyer
John N. Dyer,
Dean of Science and Engineering

ABSTRACT

An analytic model is developed to allow derivation of the probability that a molecule in the atmosphere of Saturn's rings collides with at least one ring particle when traversing the ring plane. The resulting expression involves details of the molecule's trajectory, including the velocity of the molecule relative to ring particles; thus, the theory is compatible with recently developed ballistic-transport computer models used in the analysis of the rings. The collision theory is applied to the case of a low energy, isotropic molecular production process to make inferences on the spatial extent of the ring atmosphere associated with such a source. The high frequency of collisions expected for the atmosphere in the vicinity of the A and B rings suggests a toroidal atmosphere.

TABLE OF CONTENTS

LIST OF SYMBOLS

b	thickness of a sublayer of a "slab" whose overall thickness is h ($h < b$)
h	thickness of the translating slab (containing particles) through which a molecule passes (corresponds to ring thickness in application of the collision theory)
$n(r)$	number density of particles in a slab (or in the ring for applications of the collision theory)
r	particle radius (sometimes referred to in this paper as the "size" of a particle)
$\vec{v}_{ej}$	ejection velocity of a molecule, relative to its source particle
$\vec{v}_m$	velocity of a molecule
$\vec{v}_p$	velocity with which the slab translates (equivalent to a representative) velocity of the particles "contained" in the slab
D_I	distance that the slab translates in time t
L	scale length for the extent of the slab in directions normal to its thickness
N	equilibrium number of molecules (of a given type) in ring atmosphere deriving from a specific production mechanism
$N(r_i)$	number of slab (ring) particles of size r_i, contained in the slab (meaningful only for discretely distributed r)
P_c	probability that a molecule collides with at least one ring particle during a given passage through the slab (ring)
$P_{no}(r_i)$	probability that a molecule passes through the slab (ring) without colliding with a particle of size r_i (only strictly meaningful for discrete r)
$P_{no(j)}$	probability that j particles of size r_i are not in the collision region

$Q_e(r,\lambda)$ extinction cross section, sometimes referred to as the extinction coefficient (relates to the effective size of a particle with regard to removal of electromagnetic energy from a beam via scattering and absorption)

R orbital radius (see Section III)

R_I interaction radius (see Appendix B)

S sticking coefficent (the probability that a molecule will adhere to a surface when it collides with that surface)

T a "mean" orbital period typical of the trajectories of all molecules of a certain type produced by a given process

T_p number of completed orbital periods

W production rate (of molecules) associated with a specific mechanism, usually including only those molecules which assume closed orbits

α,β,γ direction cosines which specify a molecule's path as it passes through the slab, when working in a frame of reference in which the slab translates at $\vec{v}_p$ (see Figure 2)

α',β',γ' direction cosines which specify a molecule's path through the slab, when working in a frame of reference in which the slab is fixed (see Figure C2)

ϕ angle used to describe the deviation of the actual direction of $\vec{v}_p$ from the assumption that $\vec{v}_p$ is constant

λ wavelength (of electromagnetic radiation)

μ angle that an electromagnetic beam makes with the surface normal of a slab (ring)

θ angle in the x-y plane between the projection of the molecular path and the +x direction ($\vec{v}_p$ direction), defined in a frame of reference in which $\vec{v}_p \neq 0$, referred to in this paper as the "orbital aximuth"

θ' same as θ, except defined in the frame of reference with $\vec{v}_p = 0$

ACKNOWLEDGMENT

The author expresses his appreciation to Professor Robert Armstead, whose scholarly advice helped him over the mental obstacles encountered in the conceptualization of this thesis.

A special thanks is also extended to his wife, Deborah, for her abundant patience and support.

I. INTRODUCTION

It has been well established that the particles of which Saturn's rings are composed are primarily water ice (Cuzzi et al., 1984). Accepting this, one would expect that various erosive processes would produce a ring atmosphere comprised of H_2O molecules and their constituents, e.g., H atoms. The density of such an atmosphere would be determined by balancing the production rates (of atoms and molecules) associated with the erosion mechanisms with losses resulting from capture by Saturn, escape from the Saturnian system, and recapture by the ring particles.

Early theoretical estimates of a ring atmosphere (Dennefeld, 1974; Blamont, 1974) considered sources such as sublimation, meteroid impact, and bombardment by solar and interstellar wind.[1] These analyses were concerned only with the atmosphere associated with the A and B rings (see Figure 1), by far the most significant potential sources of material for a ring atmosphere, owing to their large masses (Appendix A gives a summary of ring nomenclature and dimensions). Dennefeld calculated the density of the H_2O atmosphere to be ~25 cm^{-3}, the molecules confined to a toroidal region closely surrounding the A and B rings. He estimated the H atom

---

[1]Dennefeld presented a conceptual model for the study of ring atmospheres, which is of fundamental importance. This model is discussed later in this section.

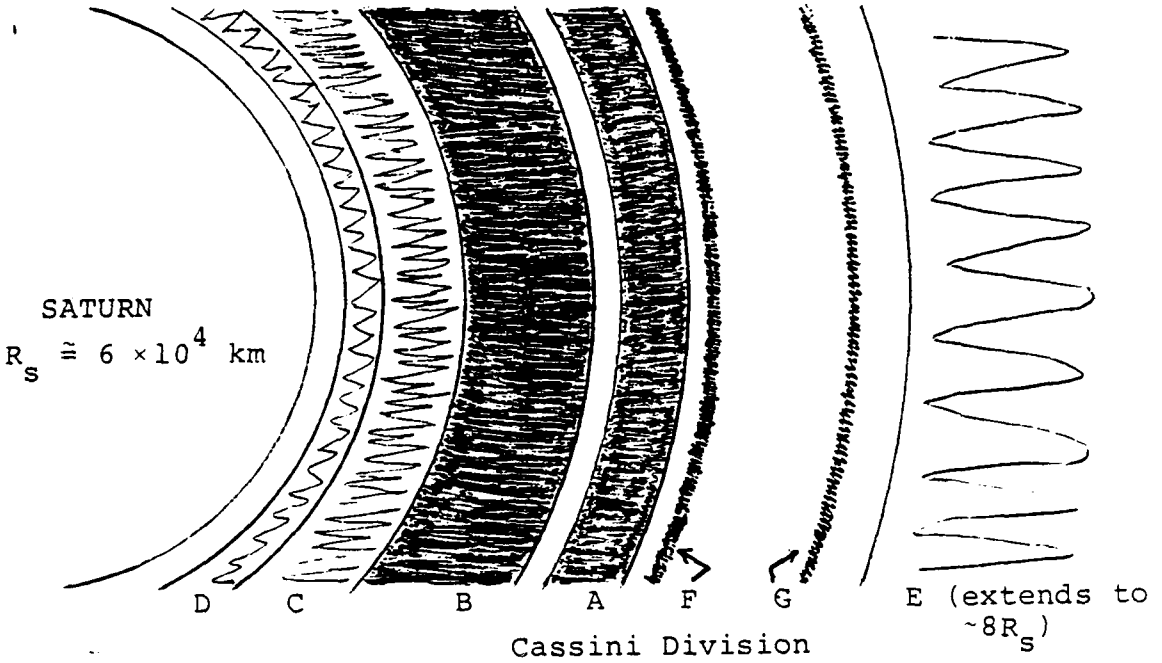

Figure 1. Nomenclature of the Saturnian Ring System (drawn to scale)

component of the atmosphere to have a density of ~1 cm^{-3} distributed through a sphere of ~3×10^5 km, well beyond the outside edge of the A ring.

Schemes for detection of the atmosphere all rely on measurement of H Lyman-α emission from the vicinity of the rings, the most sensitive means available. Thus, analysis is limited to the neutral H atmosphere. Using this approach, several researchers put Dennefeld's estimates to the test. Observations from instruments onboard rockets (Weiser et al., 1977), satellites (Barker, et al., 1980; Clarke, 1981),

Pioneer II (Judge et al., 1980), and Voyager I (Broadfoot et al., 1981) detected H atoms near the A and B rings. Results were reasonably consistent, suggesting a H density 2-3 orders of magnitude greater than Dennefeld predicted. The shape of the atmosphere (spherical versus toroidal) cannot be conclusively deduced from these Lyman-α measurements, but preliminary analysis of Voyager data indicates that it does not extend beyond the outer edge of the A ring (Cuzzi et al., 1984).

Efforts to reconcile theoretical estimates of the H atmosphere with observations have primarily been directed toward proposing new sources or re-evaluating those previously considered. Proton flux from Saturn's ionosphere (Ip, 1978), photodissociation of H_2O on the ring particles (Carlson, 1980), magnetospheric ion sputtering (Cheng et al., 1978,1980), and meteroid impact (Morfill et al., 1983; Ip, 1983) are among the most seriously studied erosive mechanisms.[2] Of these meteroid impact appears likely to be the dominant source.

While understanding of the ring atmosphere has increased, Dennefeld's conceptual model has remained the foundation for its theoretical analysis. It is worthwhile to review this model. Suppose that a particular erosive process produces atmospheric molecules (e.g., H_2O or H) with these molecules

---

[2]Some have also considered H atom sources external to the rings such as atoms escaping from Saturn's atmosphere (Shemansky and Smith, 1982). Preliminary calculations indicate that this process may be quite significant.

having some initial velocity distribution. The trajectory of each molecule is primarily governed by its gravitational interaction with Saturn, the dominant central body in the Saturnian system. If the ring atmosphere is quite tenuous, collisions between molecules as they move in their Keplerian orbits is unlikely (this assumption poses no problem for Saturn's rings, since for a density of even 1000 cm^{-3} the mean free path is $\sim 10^7$ km). A molecule's initial velocity and position within the ring determines its orbit for which there are three possible cases[3]:

(1) the trajectory takes the molecule into Saturn's atmosphere, thus removing it from the ring atmosphere.

(2) the orbit is open (hyperbolic) with the molecule escaping the entire Saturnian system.

(3) the orbit is elliptic with the molecule passing through the ring once or twice during each orbital period (depending on the eccentricity of the orbit).

For those molecules with elliptic orbits, some will be lost from the atmosphere to the rings. The probability that this occurs during each passage of a molecule through the rings is the product of the probabilities of its colliding with ring particles and of its sticking to a particle during this process. The spatial extent of the atmosphere tends to be toroidal if the initial speed of the molecules relative to the orbital speed of the ring particles is small. On the

---

[3]The first two cases apply if the erosive mechanism produces molecules with high speeds relative to the ring particles; the third is dominant for relatively lower energy processes.

other hand if the initial speed is much greater than that of the ring particles, then the atmosphere will tend to be more spherical. A mathematical expression of this process of the form introduced by Dennefeld is

$$N = \frac{WT}{SP_C} ,$$

where:

$N \equiv$ number of molecules (of a given "kind") in the equilibrium atmosphere (from a specific production mechanism).

$W \equiv$ production rate (sec^{-1}) of molecules associated with a specific mechanism which assume elliptic orbits (call this the "source term").

$T \equiv$ mean orbital period (sec); this term incorporates initial velocity information, so it might more generally be referred to as the "ballistic term."

$S \equiv$ sticking coefficient, the probability that a molecule will adhere to a ring particle when it collides with it.

$P_C \equiv$ probability that the molecule collides with a ring particle as it passes through the ring.[4]

This model is admittedly crude, but it does contain the essence of the physical system. To see how the theory has evolved, each term is discussed below.

---

[4] A tacit assumption in this formulation is that the average trajectory intersects the ring only once during an orbital period. If it passes through the ring twice during a period, P_C hasa slightly different interpretation, but the other terms are unaffected.

The source term, W, has received much attention as discussed in some detail earlier.

The ballistic term, T, is receiving increased emphasis. Ballistic transport models (Durisen, 1984; Ip, 1983) incorporate inhomogeneities found in the macrostructure of the rings with improved estimates of initial velocity distributions to allow better specification of molecular trajectories.

The sticking coefficient, S, is probably the least understood factor in the theory. The physical chemistry underlying the phenomenon is not well developed, while laboratory experiments do not appear to accurately replicate conditions found in the ring environment.[5] While it may be possible that the physical chemistry problem will be solved, a more basic dilemma will likely remain for quite some time: S cannot be determined accurately unless detailed knowledge of individual ring particles is developed. Specifically, impurity levels and the phase of the water ice in the particles are poorly known (Weidenschilling, 1984), and the surface texture of the particles is still being debated (Kerr, 1985).

Another feature of the model, which has received little attention is the collision probability, P_C. In the literature

---

[5]For example, Carlson (1980) used S = 0.22 for collisions involving H atoms, based on experiments (Brackmann and Fite, 1961) in which a H beam impinged upon a liquid-nitrogen-cooled copper plate. The beam was so dense that recombination of atoms to produce H_2 was a significant source of loss of the atoms from the beam. This experiment does not appear to closely approximate the physical system.

P_c is consistently expressed as a function of the optical thickness, τ, the definition of which is discussed in Section III.B. Dennefeld set P_c equal to τ, while recent works (Carlson, 1980; Ip, 1983) use

$$P_c = 1 - e^{-\tau} .$$

This seems to be a simplification of the collision process, since one would expect P_c to depend on such trajectory-related factors as velocity of the molecule relative to the ring particles at the location of passage, and the path length through the ring (Durisen (1984) states that P_c will depend on optical thickness, and the "slant path of an ejectum through the rings," but does not elaborate). Also, the above expressions for P_c do not account for multiple collisions during one passage through the rings by a molecule.[6] The existence of multiple collisions, if significantly probable, has implications both for density of the atmosphere (there are more "sticking" opportunities), and for its spatial distribution.

The aim of this paper is to elevate the theory of collisions between ring particles and atmospheric molecules to a level of sophistication on par with that of ballistic

---

[6]Note that nowhere in Dennefeld's model are multiple collisions considered. The impact of this omission is discussed later.

transport models now utilized in the study of ring atmospheres. A generalized model for determining P_c is developed in Section II, while in Section III its applicability to the actual ring environment is discussed. Section IV is a mathematical analysis of the expression derived for P_c. Finally, in Section V the theory is applied to the special case of low energy, isotropic production processes (e.g., sublimation) to illustrate inferences that can be made on the spatial extent of the ring atmosphere, based on the frequency of collisions.

II. THEORY

In this section, the general problem of a molecule passing through a translating target consisting of randomly distributed macroscopic particles is addressed. The probability that it collides with at least one particle is calculated.

Consider a region in space of large extent, L, in two dimensions, and of a smaller thickness, h. This slab is populated by noninteracting spherical particles which are randomly distributed (spatially) and fixed with respect to the slab. Assume that the size of the spheres is limited to radii in the interval $[r_{min}, r_{max} << h]$ upon which the radii may be distributed either discretely or continuously. The number density of particles of size r is denoted by n(r).[7] Finally, the slab as a whole translates in a direction normal to its thickness with constant velocity, $\vec{v}_p$.

Now suppose that a molecule traveling along a straight path with speed v_m passes through the slab. Assume that the molecule is much smaller than the smallest particle in the slab, and that it only interacts with the particles through mechanical collision. The relationship between the molecule

---

[7] For discrete distributions n(r) has units m^{-3}. For continuous distributions it has units m^{-4}, so that n(r)dr is interpreted as the number of particles per m^3 in a radius increment [r,r+dr].

and the slab can be conveniently described using direction cosines as shown in Figure 2(a). Notice that the x-axis is chosen to be parallel to $\vec{v}_p$.

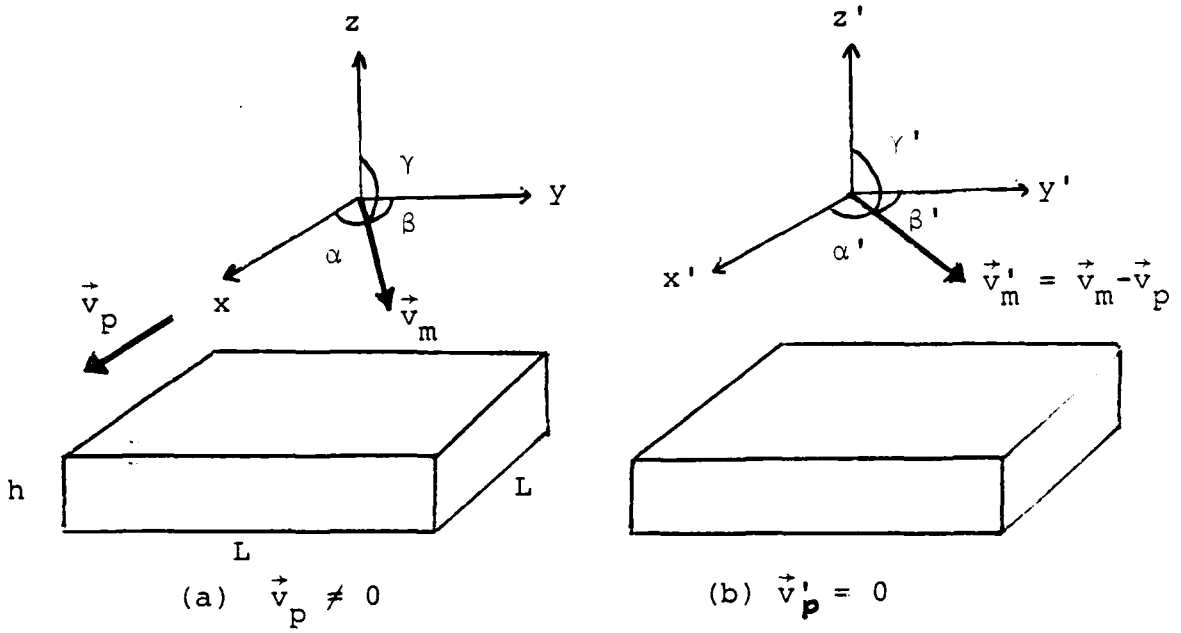

(a) $\vec{v}_p \neq 0$ (b) $\vec{v}'_p = 0$

Figure 2. Alternate Frames of Reference

Calculation of the probability of the molecule colliding with at least one particle as it passes through the slab, henceforth denoted as P_c, can be accomplished in the frame of reference shown in Figure 2(a). This procedure, however, is mathematically tedious (see Appendix B). The problem is simplified by converting to a frame of reference in which v_p equals zero (Figure 2(b)). This approach is detailed below.

Suppose that the conversion to the frame of reference with v_p equal to zero has already been accomplished (see

Appendix C for details). For simplicity, let the path of the molecule be normal to the slab, i.e., γ' equals zero, and n(r) be discrete (extension of the results for this case will be generalized to cases with continuous r and arbitrary molecular path). The molecule will collide with any particle of radius r_i which has its center anywhere in the cylindrical volume (collision region) whose axis coincides with the molecule's path as shown in Figure 3.[8] The probability

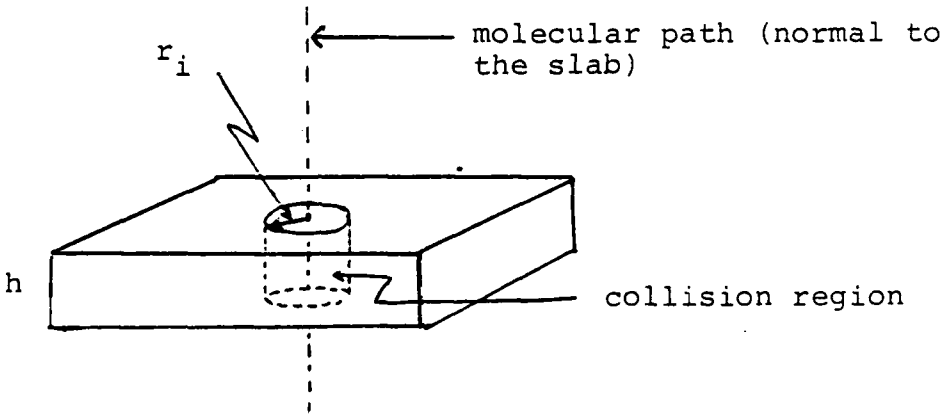

Figure 3. Collision Region for Particles of Radius r

that a collision does not occur with particles of size r_i is equivalent to the probability that no particles of that

---

[8]Note that it was tacitly assumed that the molecule is essentially a point mass. This enables one to define the collision region as was done above. An equivalent way to conceptualize the collision cylinder is to let the molecule have radius r, and the particles be point masses. The molecule then collides with any particles it "sweeps out" along its path. Of course the resulting collision region again is a cylinder of radius r.

size have centers in the collision region. Denote this probability as $P_{no}(r_i)$. Since the particles were assumed to not interact, the $P_{no}(r_i)$ for all i are mutually independent. This allows one to write for discrete r:

$$P_c = 1 - \prod_i P_{no}(r_i), \quad \text{over all } r_i . \qquad \text{(II.1)}$$

The problem is to find an expression for $P_{no}(r_i)$.

Under the assumptions of the model, the uniform probability distribution governs the location of each particle, i.e., the probability that a particle will be found in some portion of the slab is proportional to the volume of that portion. For example, consider one particle of size r_i. The probability that it is not in the collision region is

$$P_{no(1)} = \frac{L^2h - \pi r_i^2 h}{L^2h} ,$$

where the numerator is volume of the slab minus the collision region, and the denominator is the volume of the slab. Since the location of each particle in the slab is independent of the location of other particles, the probability that any two specific particles of size r_i are not in the collision region is

$$P_{no(2)} = \left(\frac{L^2h - \pi r_i^2 h}{L^2h}\right)^2 .$$

Extending this line of reasoning, it is clear that

$$P_{no}(r_i) = \left(\frac{L^2h - \pi r_i^2 h}{L^2 h}\right)^{N(r_i)} ,$$

where:

$$N(r_i) = n(r_i)L^2h$$

is the total number of particles with radius r_i in the slab. $P_{no}(r_i)$ can be rewritten as

$$P_{no}(r_i) = \left(1 - \frac{\pi r_i^2 n(r_i) h}{N(r_i)}\right)^{N(r_i)} \qquad \text{(II.2)}$$

If $N(r_i)$ is large, then

$$P_{no}(r_i) \cong \exp\{-\pi r_i^2 n(r_i) h\} . \qquad \text{(II.3)}$$

Substituting into equation (II.1) with $N(r_i)$ large for all r_i yields

$$P_c = 1 - \prod_i \exp\{-\pi r_i^2 n(r_i) h\}$$

or

$$P_c = 1 - \exp\{-\pi h \sum_i r_i^2 n(r_i)\} , \qquad \text{(II.4)}$$

recalling that r is discretely distributed, and the molecular path is normal.

Extending this result to the case when the molecule's path makes an angle γ' with a normal from the slab is easily accomplished. Notice that the only difference between this case and that of the normal path is that the length of the molecular path (hence the length of the collision cylinder) increases from h to $h/|\cos \gamma'|$. Therefore,

$$P_c = 1 - \exp\{\frac{-\pi h}{|\cos \gamma'|} \sum_i r_i^2 n(r_i)\} \qquad \text{(II.5)}$$

with r discrete and the molecular path not necessarily normal.

Extension to the case when r is continuous is affected by replacing the summation in equation (II.5) with integration (see the first footnote on page 9 to see the new interpretation required for n(r)). This yields

$$P_c = 1 - \exp\{\frac{-\pi h}{|\cos \gamma'|} \int_{r_{min}}^{r_{max}} r^2 n(r) dr\} , \qquad \text{(II.6)}$$

where r is continuous and the molecular path is not necessarily normal to the slab.

Equations (II.5) and (II.6) represent solutions to the problem when working in a frame of reference for which v_p equals zero. Often problems are not initially formulated in this particular frame. Appendix C shows how to convert

these results back to the original frame of reference (shown in Figure 1). Substituting from equation (C.8) yields

$$P_c = 1 - \exp\left\{\frac{-\pi h}{|\cos\gamma|}\sqrt{1-2\left(\frac{v_p}{v_m}\right)\cos\alpha+\left(\frac{v_p}{v_m}\right)^2}\sum_i r_i^2 n(r_i)\right\} \qquad \text{(II.7)}$$

for r discrete, and

$$P_c = 1 - \exp\left\{\frac{-\pi h}{|\cos\gamma|}\sqrt{1-2\left(\frac{v_p}{v_m}\right)\cos\alpha+\left(\frac{v_p}{v_m}\right)^2}\int_{r_{min}}^{r_{max}} r^2 n(r)\,dr\right\} \qquad \text{(II.8)}$$

for r continuous. Equations (II.7) and (II.8) are more convenient than equations (II.5) and (II.6) for some applications. It is interesting to note that while the length of the molecular path in the frame of reference with $\vec{v}_p$ not equal to zero is $h/|\cos\gamma|$, the "effective path length," pertinent to the collision problem, is

$$L_{eff} = \frac{h}{|\cos\gamma|}\sqrt{1-2\left(\frac{v_p}{v_m}\right)\cos\alpha+\left(\frac{v_p}{v_m}\right)^2}\,, \qquad \text{(II.9)}$$

which accounts for the relative motion of the molecule versus the ring particles.

Equations (II.5)-(II.8) represent the fruition of this derivation of P_c. Table 1 gives a review of the tacit and explicit assumptions of the model.

TABLE 1

ASSUMPTIONS OF THE THEORETICAL MODEL

Assumptions	Comments
spherical particles	mathematically convenient
random spatial distributions of the particles	justifies using the uniform probability density function
$h < L$	facilitates application of the model to the rings
$r_{min} \leq r \leq r_{max}$	no significance beyond "quantifying" particle size
$r_{max} << h$	effectively excludes collisions outside the nominal confines of the slab
$r_{min} >> r_{molecule}$	allows the molecule to be treated as a point particle
molecule enters and leaves slab through its large (area of L^2) faces	facilitates application of the theory to the rings
slab translates with velocity, v_p, normal to its thickness, h	facilitates application of the theory to the rings,
$\vec{v}_p$ and $\vec{v}_m$ constant	mathematically convenient
particles fixed relative to the slab	mathematically convenient
number of particles in the slab is large	justifies exponential approximation in probability calculation

Is the theoretical model utilized here relevant to conditions in Saturn's rings? This question is discussed in the next section.

III. APPLICATION TO SATURN'S RINGS

A. APPLICABILITY OF THE THEORETICAL MODEL

1. General Comments

Before proceeding with analysis of collisions between ring particles and atmospheric molecules, the validity of the generalized "slab" model of Section II must be established vis-à-vis the actual ring environment. The essential assumptions[9] of the model are:

(1) the particles in the slab are spherical.

(2) the radius (size) of any particle in the slab is in an interval $[r_{min}, r_{max}]$ where r_{min} is much greater than the size of the molecule and r_{max} is much smaller than the slab thickness, h.

(3) the spatial distribution of particles within the slab is random, i.e., the location of each particle is governed by the uniform probability density function with all particles mutually independent (in a statistical sense).

(4) the number of particles within the slab is large enough for the exponential approximation (equation (II.3)) to be valid.

(5) the velocity of the slab, $\vec{v}_p$, is constant.

(6) the velocity of the molecule, $\vec{v}_m$, is constant.

(7) the slab particles are fixed relative to the motion of the slab as a whole.

---

[9] Some of the assumptions listed in Table 1 were adopted to facilitate application of the model to the rings. These assumptions have no physical significance, so they are not discussed here.

If a "physical slab" can be defined in the rings which reasonably satisfies the above conditions, then the applicability of the model is verified. Note, however, that the physical slab is an abstract concept, since it is related to the passage of a specific molecule, on a specific trajectory.

To facilitate the discussion of the above seven assumptions, they can be divided into three categories, those related to:

(1) particle properties (assumptions (1) and (2)).

(2) particle distribution properties (assumptions (3) and (4)).

(3) velocity-related properties (assumptions (5)-(7)).

Below each of these categories is discussed with respect to Saturn's A and B rings. The other rings will not be considered, since they are not expected to contribute much to the ring atmosphere (owing to their low masses). Observational data referenced in Section I supports this exclusion.

2. Particle Properties

Individual ring particles have not yet been observed, thus absolute verification of the assumption of spherical shape cannot be accomplished. However, such a shape is adopted ubiquitously in the development of ring models. Observational data does not suggest that this traditional approach is invalid (Weidenschilling et al., 1984), in fact the Voyager radio occultation experiment (Tyler et al., 1983) eliminates the possibility of very elongated particles.

Therefore, at present the most reasonable shape to attribute to ring particles is spherical.

Most ring particles have sizes in a continuous radius interval (Cuzzi et al., 1984; Esposito et al., 1984; Weidenschilling et al., 1984)

$$1 \text{ cm} \lesssim r \lesssim 5 \text{ m} .$$

Clearly, r_{min} is much greater than the size of a H_2O or H molecule. The thickness, h, of the A and B rings is nominally not larger than 200 m, but locally may be as small as 10 m (Cuzzi et al., 1984). The requirement that r_{max} be much less than h should not create a problem for application of the collision theory.

3. Spatial Distribution of the Ring Particles

The simplest way to describe the rings is as a collection of mutually colliding particles whose trajectories are dominated by the gravitational influence of Saturn. Under such conditions the notion of a completely random particle distribution throughout the rings is reasonable. The physical slab could then be defined as any translating region containing the molecular path, provided that the velocity-related assumptions are valid for that specific region. Choose the largest such region consistent with the other assumptions to be the physical slab. As will be shown in the discussion of velocity-related requirements, this region

will have a considerable volume. This is desirable, for even if n(r) is quite small (as limited measurements have indicated (Marouf et al., 1983)), the requirement that the number of particles in the slab be large is likely to be satisfied.

In actuality the rings exhibit considerable fine structure (i.e., variations in optical thickness) on radial scales down to ~1 km (Esposito et al., 1984). Apparently the primary cause of this fine structure is linked to the gravitational effects of other bodies in the Saturnian system, especially the moons. Gravitational resonances are responsible for the creation of zones where stable particle orbits are precluded (e.g., the Cassini Division), and may generate density waves within the rings. The net effect of fine structure on the collision theory is to limit the scale over which random spatial particle distribution is correct. This can be best understood by considering the following examples.

In the first example, the slab is divided into two regions as shown in Figure 4. Suppose that the particles in

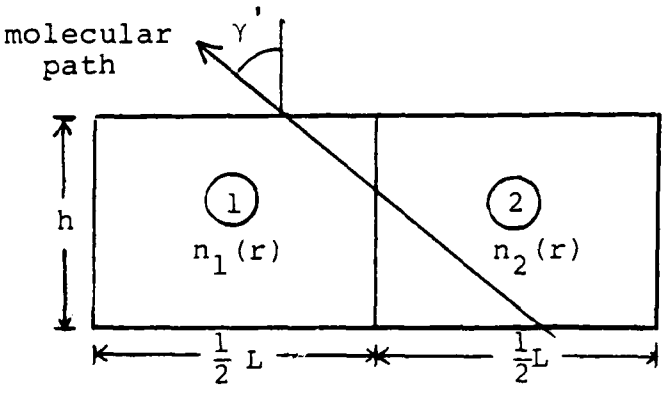

Note: For simplicity, consider the frame of reference with $\vec{v}_p = 0$, and require the molecular path to be parallel to a slab edge.

Figure 4. Model for Analyzing the Effect of Nonrandom Particle Distribution

each region are constrained to remain within that region; this represents the departure from truly random spatial distribution of the particles. Let $n_1(r)$ equal $n_2(r)$ with r discrete. What is the probability that the molecule suffers at least one collision when passing through the entire slab? Attack this problem by reformulating it as passage through two smaller slabs shown in Figure 5 as shaded regions.

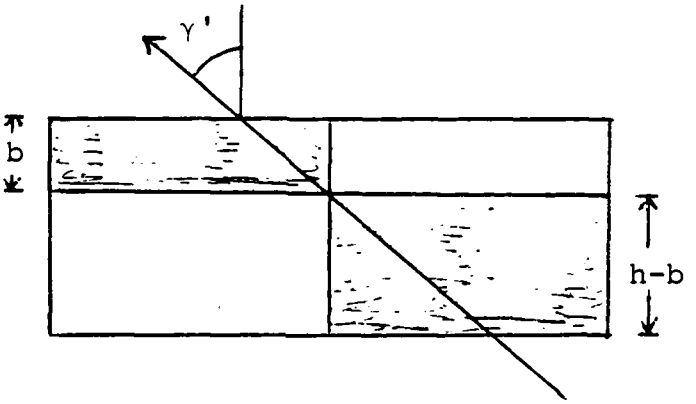

Figure 5. The Two Slabs used in Reformulating the Problem

From Section II, the probability of no collision with particles of size r_i for the slab of thickness b is

$$P_{no(b)}(r_i) = \left(1 - \frac{\pi r_i^2 n(r_i)\left(\frac{b}{|\cos \gamma'|}\right)}{N(r_i)}\right)^{N(r_i)} ,$$

where:

$$N(r_i) = n(r_i)L^2 b .$$

For all r_i this becomes

$$P_{no(b)} = \prod_i \left(1 - \frac{\pi r_i^2 n(r_i) \left(\frac{b}{|\cos \gamma'|}\right)}{N(r_i)}\right)^{N(r_i)}$$

which for large $N(r_i)$ becomes

$$P_{no(b)} = \prod_i \exp\left\{-\pi r_i^2 n(r_i) \left(\frac{b}{|\cos \gamma'|}\right)\right\}$$

$$= \exp\left\{\frac{-\pi b}{|\cos \gamma'|} \sum_i r_i^2 n(r_i)\right\} . \qquad \text{(III.1)}$$

Similarly, for the slab of thickness (h-b)

$$P_{no(h-b)} = \exp\left\{-\frac{\pi (h-b)}{|\cos \gamma'|} \sum_i r_i^2 n(r_i)\right\} \qquad \text{(III.2}$$

for $n(r_i)L^2(h-b)$ large. The probability of collision [illegible] entire passage through the original slab is

$$P_c = 1 - P_{no(b)} P_{no(h-b)} .$$

Substitution yields

$$P_c = 1 - \exp\left\{\frac{-\pi b}{|\cos \gamma'|} \sum_i r_i^2 n(r_i)\right\} \exp\left\{\frac{-\pi (h-b)}{\cos \gamma'} \sum_i r_i^2 n(r_i)\right.$$

or

$$P_c = 1 - \exp\{\frac{-\pi h}{|\cos \gamma'|} \sum_i r_i^2 n(r_i)\} \quad . \qquad \text{(III.4)}$$

This result is the same as that obtained when a random spatial distribution over the entire slab is assumed. Careful consideration reveals an important qualification to this conclusion. Notice that the assumption of exponential form is less tenable in the "nonrandom" case, since there it is required that both $n(r_i)L^2b$ and $n(r_i)L^2(h-b)$ be large, while in the completely random case $n(r_i)L^2h$ must be large. Extending this line of reasoning to cases where the original slab is further subdivided into regions to which the particles are confined, it is clear that at some point the exponential approximation will certainly fail.

In the second example, the slab is again divided into two regions (Figure 4), but now $n_1(r)$ is not equal to $n_2(r)$. Following the approach taken above, the collision probability is

$$P_c = 1 - \exp\{\frac{-\pi b}{\cos \gamma'|} \sum_i r_i^2 n_1(r_i)\} \exp\{\frac{-\pi(h-b)}{|\cos \gamma'|} \sum_j r_j^2 n_2(r_j)\} \quad ,$$

or

$$P_c = 1 - \exp\{\frac{-\pi}{\cos \gamma'|}[b \sum_i r_i^2 n_1(r_i) + (h-b) \sum_j r_j^2 n_2(r_j)]\} \quad , \qquad \text{(III.5)}$$

where both $n_1(r_i)L^2b$ and $n_2(r_j)L^2(h-b)$ must be large enough to justify the exponential approximation. The collision theory is here valid in principle, but its application is more difficult.

From this point on, the A and B rings will be assumed to satisfy the spatial distribution conditions. However, it must be kept in mind that fine structure effects may interject inaccuracies into calculations.

4. Velocity-related Assumptions

Reviewing, the three velocity-related assumptions are: $\vec{v}_p$ is constant; $\vec{v}_m$ is constant; and the particles in the slab are fixed relative to $\vec{v}_p$. Each in turn is addressed below, but the validity of the concept of slab velocity when applied to the ring system must first be demonstrated. As discussed in Section III.A.3, choosing the physical slab to be as large as possible is advantageous. By means of a simple example, it can be shown that a single velocity well approximates the orbital motion of all of the particles in even a quite large slab (this velocity corresponds to $\vec{v}_p$). Suppose that a slab with L equal to 10,000 km is centered in the B ring as shown in Figure 6. If $\vec{v}_p$ is set equal to the particle velocity at C, $\vec{v}_c$, how much error is inherent to the system? First, consider the magnitude of $\vec{v}_c$. The location in the slab with the greatest deviation in speed relative to v_c is either point A or B. In general the orbital speed for a ring particle in the Saturnian system is

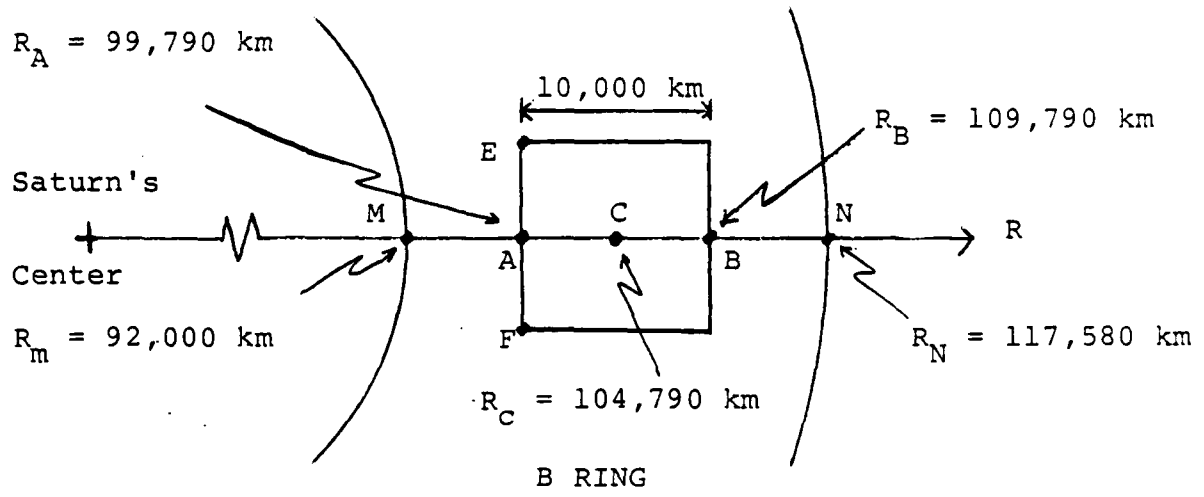

Figure 6. A Slab with L = 10,000 km Centered in the B Ring

$$v = \sqrt{GM_s/R} = \frac{6159}{\sqrt{R}} \ [\text{kms}^{-1}] \ . \qquad \text{(III.6)}$$

Applying this equation at A, B, and C yields

$$v_A = 19.496 \ \text{kms}^{-1} \ ,$$

$$v_B = 18.587 \ \text{kms}^{-1} \ ,$$

and

$$v_C = 19.025 \ \text{kms}^{-1} \ .$$

Thus, all of the particles in the slab orbit Saturn with a speed in the range [18.587 kms^{-1}, 19.496 kms^{-1}]; the greatest

deviation in assigning v_c (equals v_p) to all of the particles is 2.5%. Now, consider the direction of $\vec{v}_c$. The point of greatest deviation in direction, ϕ, occurs at point E (the angle of deviation at point F is equal to that at E). Figure 7 gives the computation of ϕ; the results given there demonstrate that the angular error in assigning $\vec{v}_c$ to all of the

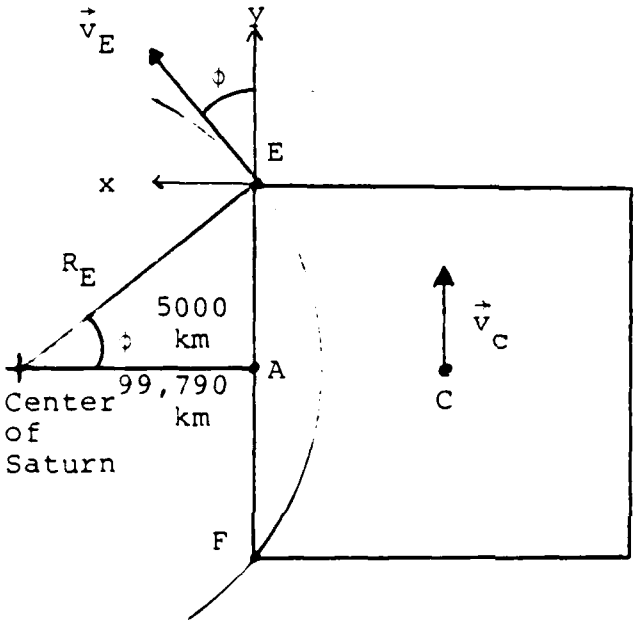

$$\phi = \tan^{-1}\left(\frac{5000}{99,790}\right)$$

$$\phi = 5.006 \times 10^{-2} \text{ rad}$$

$$R_E = 99,915 \text{ km}$$

$$|\vec{v}_E| = 19.485 \text{ kms}^{-1}$$

$$v_{Ex} = 0.975 \text{ kms}^{-1}$$

$$v_{Ey} = 19.460 \text{ kms}^{-1}$$

Figure 7. Calculation of the Maximum Angle of Deviation, ϕ

particles is quite small. The above example verifies the concept of a slab velocity, $\vec{v}_p$, for large slabs in the B ring (similar results also hold for the A ring). The concept applies even better for smaller slabs.

Accepting that $\vec{v}_p$ is a meaningful concept with regard to physical slabs in the A and B rings, the requirement that it be constant can now be examined. Once defined, the slab

will translate as shown in Figure 8. Upon reflection, the slab velocity cannot be strictly constant. Although $\vec{v}_{po}$

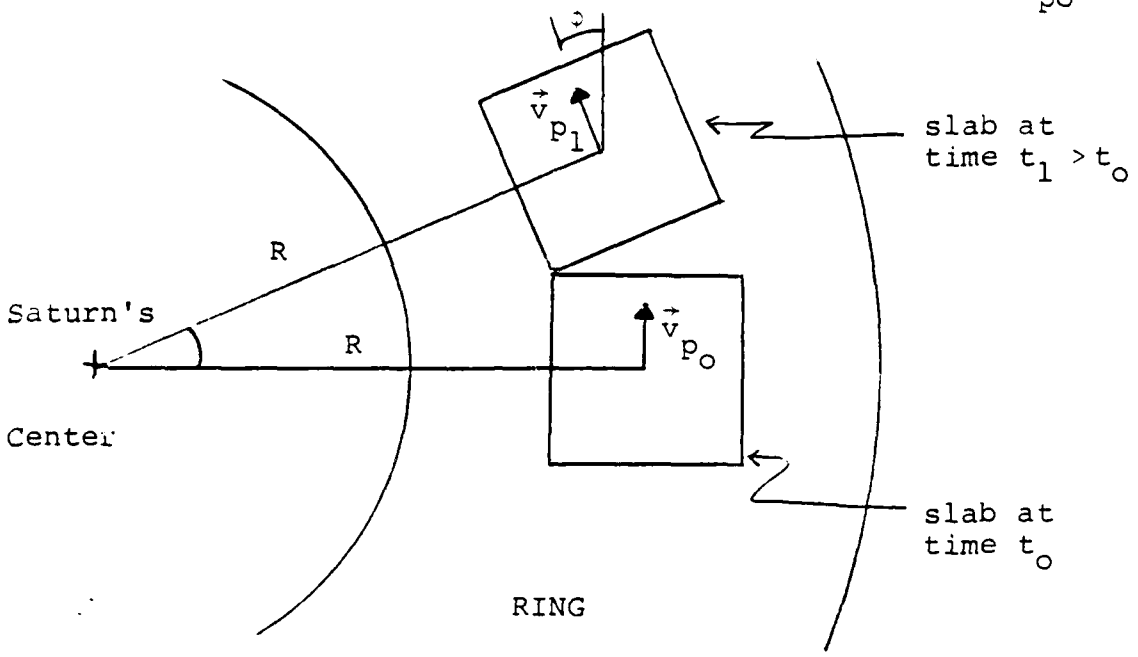

Figure 8. Translation of the Slab over Time

equals $|\vec{v}_{p1}|$, the direction of the velocity vector changes with time. The angle ϕ which quantifies the change in direction is given by

$$\phi = \frac{|\vec{v}_p|}{R} t \, . \qquad \text{(III.7)}$$

For a slab centered in the B ring (as in Figure 6),

$$\phi = 1.8156 \times 10^{-4} t \, , \qquad \text{(III.8)}$$

where t is in seconds, ϕ in radians. The time required for a variation of 1.7453×10^{-2} rad (1°) is 96.1 s. This example suggests that for the A and B rings, the assumption of constant $\vec{v}_p$ is approximately correct, if the time of passage for a molecule through the ring is short. The requirement will be met for most passages (i.e., over most γ), since the thickness of the ring is so small. To see this, then suppose that:

(1) h = 100 m,

(2) R ≅ 105,000 km (molecule passes near the center of the B ring),

(3) $|\vec{v}_m| = 20$ kms^{-1}.[10]

Over what range of γ (recall Figure 2) will ϕ be less than 1°; or phrased differently, over what range of γ will the time of passage of the molecule be less than 96 s? In general the time for passage for the molecule is

$$t = \frac{h}{v_m |\cos \gamma|} . \qquad \text{(III.9)}$$

Substituting the given information, requiring t to be equal to 96 s, and solving for γ yields

$$96 = \frac{100}{20 \times 10^3 |\cos \gamma|} ,$$

---

[10] The lowest kinetic energy of a stable orbit (measured in a frame of reference fixed with respect to Saturn) for an atmospheric particle which originates in the A and B rings, as it passes through those rings, is ~20 kms^{-1}.

$$|\cos \gamma| = 5.21 \times 10^{-3} ,$$

$$\gamma = 89.997°, 90.003° .$$

Therefore, in this representative case the range of γ is

$$0 \leq \gamma < 89.997° , \quad 90.003° < \gamma \leq 180° ;$$

virtually any γ meets the requirement.

The requirement that $\vec{v}_m$ be constant, as in the case of $\vec{v}_p$, cannot be strictly met, since the trajectory of any molecular orbit will have some curvature.[11] However, the extreme thinness of the rings allows the condition to be approximately satisfied, so this aspect of the theoretical model can be applied to Saturn's rings with no problem.

That the particles on the slab are fixed with respect to $\vec{v}_p$ cannot be strictly satisfied, either. Direct measurements of the relative velocities of the ring particles have not been accomplished, but various indirect methods yield consistent results: ~1 cms^{-1} (Weidenschilling et al., 1984). Compared to the range of orbital speeds for particles in the A and B rings

$$\underset{\text{(outer A ring)}}{16.6 \text{ kms}^{-1}} \leq v_p \leq \underset{\text{(inner B ring)}}{20.3 \text{ kms}^{-1}} ,$$

---

[11] Note that the gravitational interaction between the molecule and ring particles has been neglected, a reasonable assumption since the total mass of the rings is less than 10^{-6} that of Saturn (Null et al., 1981).

calculated using equation (III.6), the relative motion of the particles is insignificant over reasonable passage times (less than or equal to ~100 s, as discussed above). Thus, in this regard the theoretical model suffers no important restriction in applicability to the rings.

5. Summary

The above discussion has demonstrated that the conditions upon which the theoretical model is based, are generally well-satisfied in the ring environment. The only potential source of significant concern relates to assumption of random particle distribution and the validity of the exponential approximation (Section III.A.3). Unlike the other assumptions of the model, these cannot be unamibguously shown to hold for Saturn's rings. On the other hand, they cannot be shown to fail, and have considerable intuitive appeal. With this caveat noted, the theoretical model is adopted for analysis of collisions between ring particles and atmospheric molecules.

B. THE UTILITY OF OPTICAL THICKNESS IN APPLICATIONS

Having shown that the theoretical model can be viably applied to the atmosphere in the vicinity of the A and B rings, calculation of P_c using the results of Section II is justified. Since particle radius is continuously distributed, and effectively confined to an interval [0.01 m,5 m] as discussed earlier, the collision probability is (from Section II)

$$P_c = 1 - \exp\left\{\frac{-\tau h}{\cos \gamma'} \int_{0.01}^{5} r^2 n(r) dr\right\} , \qquad \text{(II.6)}$$

when working in a frame of reference with $\vec{v}_p$ equal to zero, and is

$$P_c = 1 - \exp\left\{\frac{-\pi h}{|\cos \gamma|}\sqrt{1-2\left(\frac{v_p}{v_m}\right)\cos \alpha + \left(\frac{v_p}{v_m}\right)^2} \int_{0.01}^{5} r^2 n(r) dr\right\} , \qquad \text{(II.8)}$$

when working in a frame of reference where $\vec{v}_p$ is not equal to zero. The value for h is well-constrained, while the parameters v_m, v_p, α, γ, and γ' depend on the location of a molecule's passage and its trajectory (both of which can be determined using Keplerian mechanics). If n(r) is known throughout the rings, then the calculation of P_c using the above equations will be straightforward. Although the functional form of n(r) is believed to be

$$n(r) = n_o r^{-p} , \quad p > 0 ,$$

where p may differ over r, its precise expression has only been determined for a few locations in the A and C rings (Marouf et al., 1983). Fortunately, this obstacle to the application of equations (II.6) and (II.8) can be overcome by using the concept of "optical thickness."

Optical thickness[12], τ, is defined in an operational manner: if an electromagnetic beam traverses a layer of particles at an angle μ to the layer normal, and the layer has an optical thickness of τ, then the beam's intensity is reduced by a factor of $e^{-\tau/\cos \mu}$. In general τ will depend on: particle composition, size, and shape; particle density; layer thickness; and wavelength of the incident beam. Detailed analysis of this phenomenon is beyond the scope of this paper (see van de Hulst (1981) and Chandrasekar (1960) for thorough analyses of light scattering by media consisting of small particles). However, the essential attributes of a complete analysis of τ, can be concisely summaried, generally following Cuzzi et al. (1984).

For spherical particles in a layer of thickness, h, the optical thickness is given as

$$\tau(\lambda) = \int Q_e(r,\lambda)\pi r^2 hn(r)dr \ , \qquad \text{(III.10)}$$

where:

$\lambda \equiv$ wavelength of incident radiation,

and

---

[12]Optical thickness is often referred to as "optical depth." The terms are used interchangeably in literature concerning planetary rings. Also, since τ depends on wavelength, one must be careful when comparing the results of different studies.

$Q_e(r,\lambda)$ $\equiv$ extinction cross section (a measure of the portion of incident energy removed from the beam by absorption and scattering).

When r is much greater than λ, then

$$Q_e = \begin{cases} 1, \text{ for incoherent incident radiation.} \\ 2, \text{ for coherent incident radiation.} \end{cases}$$

Considering visible wavelengths with respect to the predominant particle sizes in the A and B rings, i.e., [0.01 m,5 m], the above values for Q_e apply. Therefore, for the A and B rings the visible optical thickness when measured with an incoherent signal (e.g., stellar occultation) is

$$\tau = \int \pi r^2 hn(r) dr \ . \qquad \text{(III.11)}$$

Equations (II.6) and (II.8) can be rewritten as

$$P_c = 1 - e^{-\tau/|\cos \gamma'|} \qquad \text{(III.12)}$$

$$P_c = 1 - \exp\{\frac{-\tau}{|\cos \gamma|}\sqrt{1-2(\frac{v_p}{v_m})\cos \alpha + (\frac{v_p}{v_m})^2}\} \qquad \text{(III.13)}$$

Of course, if optical thickness measurements based on coherent, visible signals are used to compute τ, the resulting expressions for P_c will differ from equations (III.12) and (III.13) by a factor of 0.5 in the exponent of e.

Measurements of τ for Saturn's rings abound. To apply equations (III.12) and (III.13) to the rings, one must only be cognizant of the importance of the wavelength at which τ was determined. Keeping this in mind, analysis of P_c can proceed.

IV. GENERAL ANALYSIS OF THE EXPRESSION FOR THE COLLISION PROBABILITY, P_c

A. RESTRICTIONS ON THE PARAMETERS

When studying Saturn's rings, the frame of reference usually adopted features Saturn as a fixed central body orbited by ring particles following (circular) Keplerian trajectories. It is also the reference frame of most general interest when examining the ring atmosphere, since ballistic transport models are based on basic orbital mechanics. For this reason only equation (III.13) is analyzed in this section.[13]

Recall that the collision probability is given as

$$P_c = 1 - \exp\{\frac{-\tau}{|\cos\gamma|}\sqrt{1-2(\frac{v_p}{v_m})\cos\alpha + (\frac{v_p}{v_m})^2}\} \qquad \text{(III.13)}$$

Clearly P_c is a function of parameters related to the molecule's orbit (v_m,α,γ), and those that characterize the translating slab (τ,v_p). Note that α and γ are not independent, but must satisfy

$$\cos^2\alpha + \cos^2\gamma \leq 1 ,$$

---

[13] That is not to say that the reference frame with slab particles at rest is not useful in some practical applications (as is shown in Section V). Rather, although the collision problem may be solved in either frame of reference, the problem of calculating molecular trajectories is ultimately approached in the frame with $\vec{v}_p$ not equal to zero, requiring conversion to that frame.

since they are direction cosines. An alternative coordinate system which removes this interdependence specifies a molecule's path in terms of γ and θ, henceforth referred to as the "orbital inclination" and "orbital azimuth." θ is here defined as the angle between the projection of $\vec{v}_m$ in the x-y plane (the ring plane), and the x-axis (i.e., the direction in which the slab translates). Figure 9 shows the relationship between θ and the direction cosines, the mathematical expression of which is given in Appendix D. Employing the

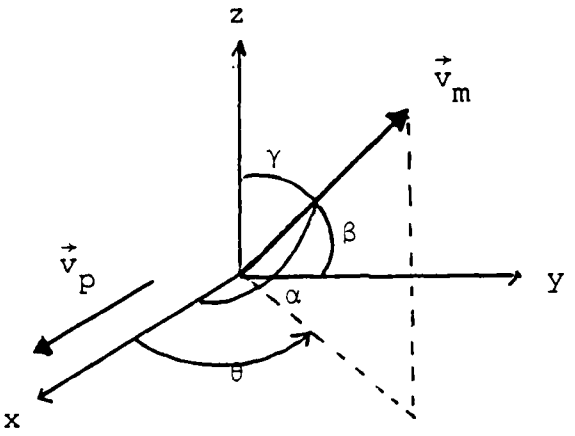

Note:

$-\pi < \theta \leq \pi$

Figure 9. Definition of the "Orbital Azimuth," θ

results of Appendix D, the collision probability can be rewritten as

$$P_c = 1-\exp\left\{\frac{-\tau}{|\cos\gamma|}\sqrt{1-2\left(\frac{v_p}{v_m}\right)\sin\gamma\cos\theta+\left(\frac{v_p}{v_m}\right)^2}\right\} . \qquad \text{(IV.1)}$$

Equation (IV.1) proves more useful than equation (III.13) in the subsequent analysis.

Before examining the expression for P_c in detail, physical considerations which limit the range of values for the parameters are outlined below. Following this, attention can then be turned to parameter values of most practical interest in the study of the atmosphere of Saturn's rings.

The optical thickness, τ, of Saturn's rings has been studied extensively. Recall from Section III.B that the measured value of τ is dependent on several variables, most importantly wavelength and coherence of the incident radiation, and the nominal size of the ring particles at the location where the electromagnetic beam is incident upon the ring plane. As shown in Section III.B, measurements based on incoherent, short wavelength (e.g., visible) radiation yield values of τ that can be most easily used in collision theory (see equations (III.11) and (III.13)). A stellar occultation experiment onboard Voyager 2 provided results that meet the above requirements (Esposito et al., 1984). Optical thickness was found to fluctuate radially, varying from:

(1) ~0.1 to ~0.4 in the C ring.

(2) ~0.7 to ~2.5 in the B ring.

(3) ~0.1 to ~0.2 in the Cassini Division.

(4) ~0.4 to ~1.0 in the A ring.

Average τ over the A-C rings is given in Appendix A. Summarizing this information, the nominal optical thickness is:

(1) 0.1 for the C ring and the Cassini Division.

(2) 1.5 for the B ring.

(3) 0.5 for the A ring.

Subsequently, in further analysis of Saturn's ring atmosphere, τ will be limited to the interval

$$0.1 \leq \tau \leq 2.0 .$$

The slab speed (which is essentially the ring particle speed in the vicinity of the molecule's path through the ring) and the molecular speed appear as a ratio, v_p/v_m, in the expression for P_c. Call v_p/v_m the "speed ratio." Estimates of H_2O molecule ejection speeds, relative to the source particle, for several production processes are:

(1) ~0.3 kms^{-1} for sublimation (Dennefeld, 1974).

(2) ~1 kms^{-1} for meteroid bombardment (Dennefeld, 1974).

Estimates for H atom ejection speed are:

(1) < 3 kms^{-1} for meteroid bombardment (Morfill et al., 1983).

(2) < 10 kms^{-1} for photodissociation of H_2O (Durisen, 1984).

Based on the above values, estimates for the speed ratio range for molecules newly ejected from particles in the A and B rings are

$$0.95 \leq \frac{v_p}{v_m} \leq 1.06$$

for H_2O molecules, and

$$0.40 \leq \frac{v_p}{v_m} \leq 1.49$$

for H atoms, noting that $\vec{v}_m$ is the sum of $\vec{v}_p$ and the ejection velocity, $\vec{v}_{ej}$. The eccentricity of the subsequent orbit, and the effect of collisions complicate precise specification of general limits on the speed ratio, but the above should suffice as guidelines. Therefore, further analysis of P_c in this paper will be limited to a range

$$0 \leq \frac{v_p}{v_m} \leq 2 .$$

By definition, γ and θ are restricted to $[0,\pi]$ and $[-\pi,\pi]$, respectively. Considering equation (IV.1), it can be seen that

$$P_c(\theta) = P_c(-\theta) ,$$

and

$$P_c(\gamma) = P_c(\pi-\gamma) \leftrightarrow P_c(\tfrac{1}{2}\pi-\gamma) = P_c(\tfrac{1}{2}\pi+\gamma) .$$

Noting these symmetries, no information is lost by limiting subsequent analysis of P_c to

$$0 \leq \theta \leq \pi ,$$

and

$$0 \leq \gamma \leq \frac{1}{2}\pi .$$

Though P_c will be analyzed over the above intervals, some physical restrictions on values for orbital inclination and azimuth are discussed in the following paragraphs.

When a given production process is considered, the initial limits on γ can easily be determined as shown in Figure 10. For example, the γ-range for H_2O is:

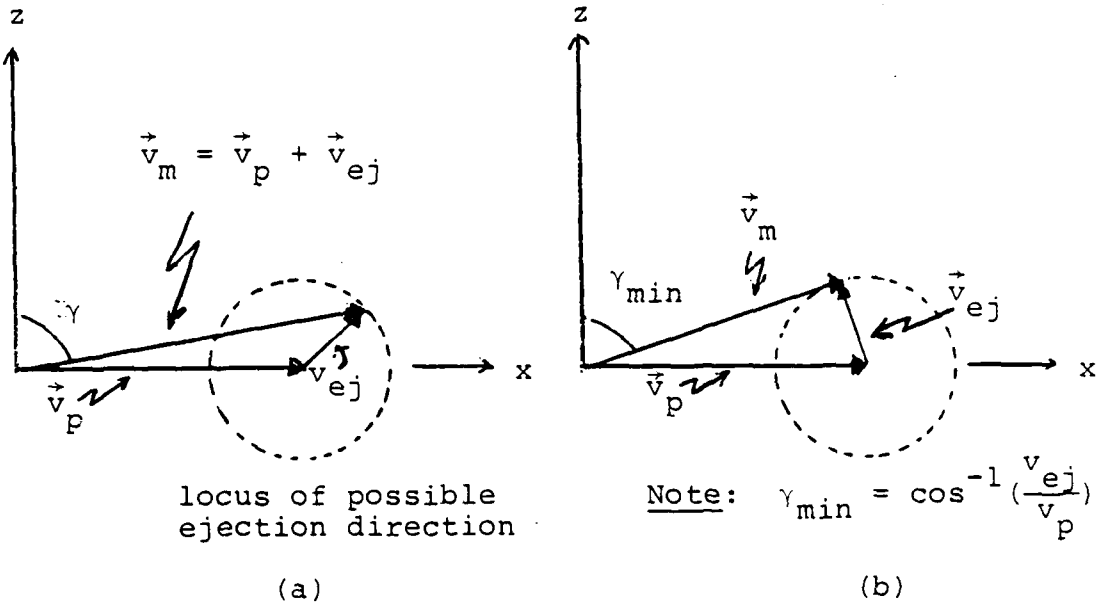

Figure 10. (a) General Relationship Between $\vec{v}_{ej}$, $\vec{v}_m$, and $\vec{v}_p$.
(b) Case for Minimum Value of γ

(1) $89° \leq \gamma \leq 91°$ for sublimation.

(2) $86.6° \leq \gamma \leq 93.4°$ for meteroid impact.

Similarly, for H atoms, γ is initially confined to:

(1) $79.6° \leq \gamma \leq 100.4°$ for meteroid impact.

(2) $53.0° \leq \gamma \leq 127.0°$ for photodissociation of H_2O on a particle surface.

As collisions occur between molecules and ring particles, the range on γ will change. If a collision is assumed to be inelastic, then upon impact the molecule will rebound with reduced kinetic energy relative to the particle. The overall effect is that γ should go to $\frac{1}{2}\pi$ as more collisions occur.

For atmospheric molecules originating on a ring particle, the initial orbital azimuth will certainly be "forward-directed," i.e.,

$$-\frac{1}{2}\pi \leq \theta \leq \frac{1}{2}\pi ,$$

as long as the ejection speed is less than the particle speed. This again follows from the fact that $\vec{v}_m$ is the vector sum of $\vec{v}_p$ and $\vec{v}_{ej}$. Subsequent collisions should not alter this assertion.

B. FUNCTIONAL DEPENDENCE ON OPTICAL THICKNESS, τ

P_c monotonically increases with increasing τ, as can be clearly observed in equation (IV.1). The rate of increase is given by (using equation (IV.1))

$$\frac{\partial P_c}{\partial \tau} = \frac{1}{|\cos\gamma|}\sqrt{1-2\left(\frac{v_p}{v_m}\right)\sin\gamma\cos\theta+\left(\frac{v_p}{v_m}\right)^2}\exp\left\{\frac{-\tau}{|\cos\gamma|}\sqrt{1-2\left(\frac{v_p}{v_m}\right)\sin\gamma\cos\theta+\left(\frac{v_p}{v_m}\right)^2}\right\}.$$

Here the effect of the other parameters on the rate with which P_c exponentially approaches one is explicitly displayed. Appendix E contains examples of the collision probability's

dependence on τ given selected values for the speed ratio, orbital inclination, and orbital azimuth.

The physical interpretation of this functional behavior is simple. Recall that for measurements at appropriate wavelengths,

$$\tau = \int \pi r^2 n(r) h dr \ .$$

If h is held constant, then higher values of τ imply greater number density, n(r). Intuitively, one would expect the collision probability to increase with increasing number density (all other things held constant), which is substantiated by the mathematical expression for P_c. Similarly, if n(r) is held constant, increasing τ implies that h must increase, the length of a molecule's path must increase, thus increasing its exposure to collision.

C. FUNCTIONAL DEPENDENCE ON THE SPEED RATIO, $\frac{v_p}{v_m}$

The behavior of the collision probability as a function of speed ratio is very interesting. Figure 11 gives a representative example of the variation of P_c as a function of v_p/v_m (see Appendix E for the results of more example calculations. For θ less than $\frac{1}{2}\pi$, a minimum for P_c occurs at v_p/v_m greater than zero. Why does this happen?

Some insight into this phenomenon can be gained by considering the partial derivative of P_c with respect to v_p/v_m, i.e.,

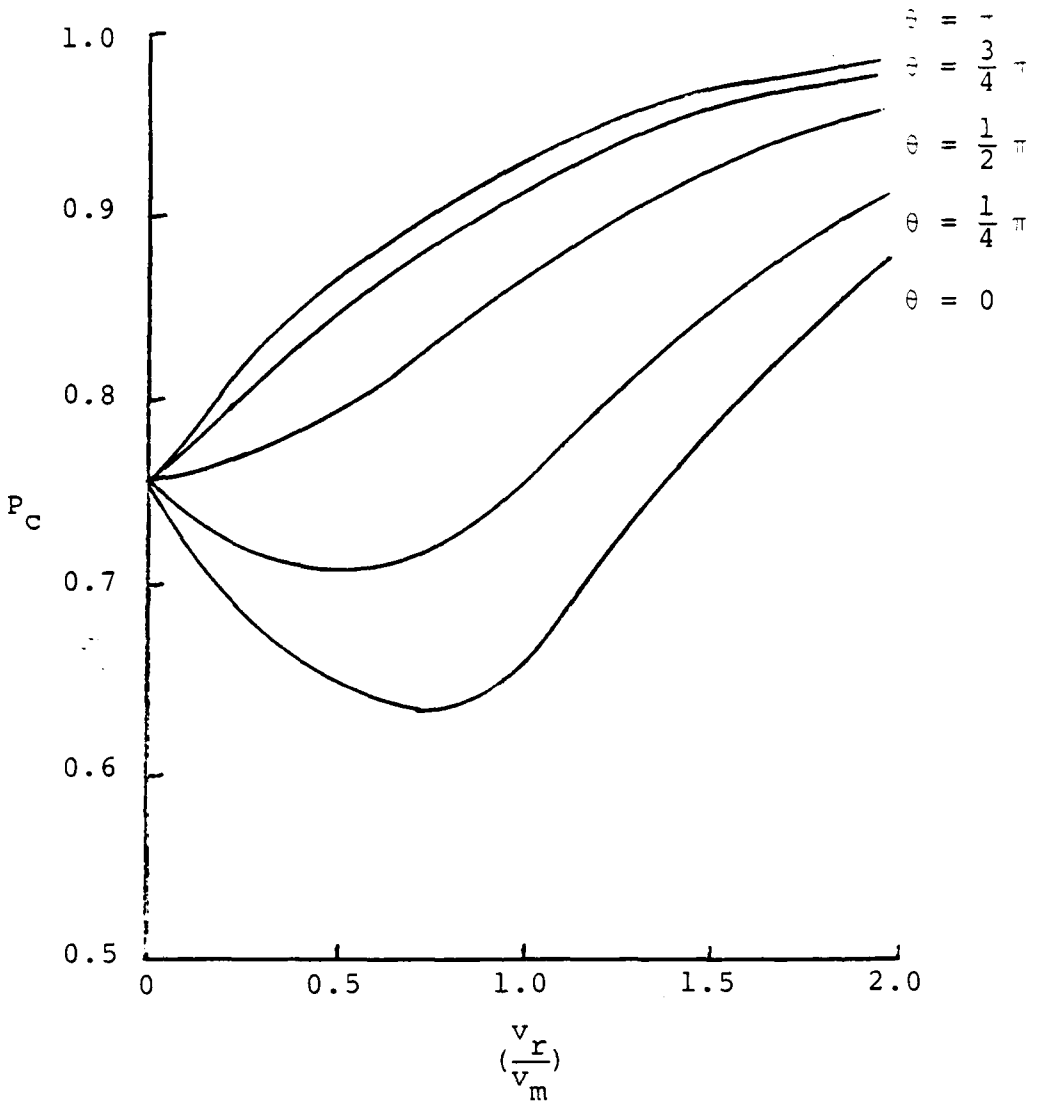

Figure 11. Collision Probability as a Function of the Speed Ratio for $\tau = 1.0$ and $\gamma = 1/4\pi$ and Various Values of θ

$$\frac{\partial P_c}{\partial (\frac{v_p}{v_m})} = \frac{\gamma}{|\cos\gamma|}\left[-2\sin\gamma\cos\theta+2(\frac{v_p}{v_m})\right]\exp\left\{\frac{-\tau}{|\cos\gamma|}\sqrt{1-2(\frac{v_p}{v_m})\sin\gamma\cos\theta+(\frac{v_p}{v_m})^2}\right\} . \quad \text{(IV.2)}$$

With all variables except v_p/v_m held constant, P_c has a minimum at

$$\frac{v_p}{v_m} = \sin \gamma \cos \theta \ . \qquad \text{(IV.3)}$$

From Appendix D, the right hand side of equation (IV.3) is identically equal to cos α, so expressing that in terms of the direction cosine gives

$$v_p = v_m \cos \alpha \ ; \qquad \text{(IV.4)}$$

a minimum of P_c occurs when the component of $\vec{v}_m$ in the direction of $\vec{v}_p$ is equal in magnitude to $|\vec{v}_p|$. Notice that relative to variation in v_p/v_m, P_c cannot assume a minimum value for speed ratio values greater than one.

Since the result of the above mathematical analysis may be difficult to reconcile with intuition. an example is given to clarify its physical meaning. Suppose that a blind mouse lives in a hole in the middle of a single-lane, one-way road. Randomly spaced steamrollers traverse this road, all moving with speed v_p. The mouse, smelling cheese in another hole a few meters down the road, dashes for that hole with speed v_m (in the same direction as the steamrollers). Given v_m, for what v_p will the mouse have the best chance to reach the cheese unharmed, neither being overtaken by a steam roller, nor running into one? The answer is that the

probability of collision is least (in this case zero) when v_p equals v_m. For v_p greater than v_m, steamrollers will tend to overtake the mouse; as v_p gets very large the probability of collision goes to one. For v_p less than v_m, the mouse will tend to run into a steamroller. The mouse's situation is analogous to that of a molecule passing through a ring. The probability of collision for the molecule is minimized when it "goes with the flow" of the particles as much as is possible. This minimum value of P_c will not in general be equal to zero for molecules passing through the ring, as it is for the mouse. This is the case, because the molecule crosses the ring plane of some angle (specified by γ).

A final comment on the influence of v_p/v_m on P_c is that

$$P_c \rightarrow 1$$

as

$$\frac{v_p}{vm} \rightarrow +\infty ,$$

regardless of the values of the other variables. For v_p very large, the ring loses its discrete character becoming essentially a continuum; collision becomes inevitable.

D. FUNCTIONAL DEPENDENCE ON ORBITAL INCLINATION, γ, AND ORBITAL AZIMUTH, ϑ

γ and ϑ specify the path of a molecule through the ring. Figures 12 and 13 show two examples of the

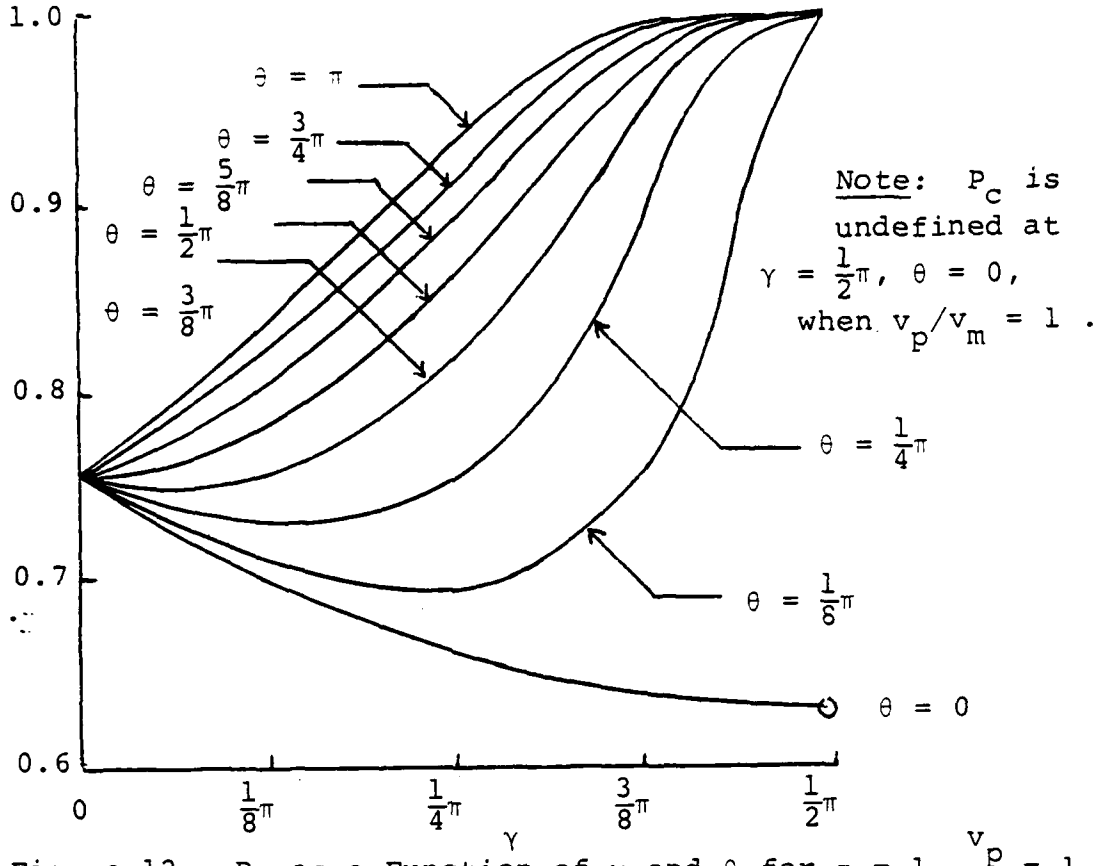

Figure 12. P_c as a Function of γ and θ for $\tau = 1$, $\frac{v_p}{v_m} = 1$

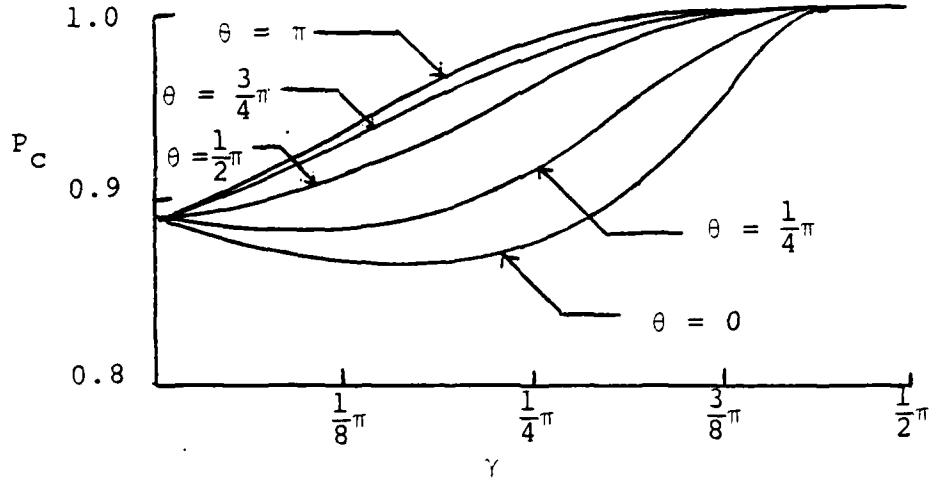

Figure 13. P_c as a Function of γ and θ for $\tau = 1$, $\frac{v_p}{v_m} = 2$

functional dependence of P_c on orbital inclination and azimuth.

First, consider the behavior of P_c with respect to θ. The partial derivative with respect to this variable is

$$\frac{\partial P_c}{\partial \theta} = \frac{\tau}{|\cos\gamma|}\left(\frac{v_p}{v_m}\right)\sin\gamma\sin\theta\left[1-2\left(\frac{v_p}{v_m}\right)\sin\gamma\cos\theta + \left(\frac{v_p}{v_m}\right)^2\right]^{-1/2} \exp\left\{\frac{-\tau}{|\cos\gamma|}\sqrt{1-2\left(\frac{v_p}{v_m}\right)\sin\gamma\cos\theta+\left(\frac{v_p}{v_m}\right)^2}\right\} . \quad \text{(IV.5)}$$

From equation (IV.5) it can be deduced that P_c is minimized when θ equals zero and maximized when θ equals π (when all other variables are held constant). As expected, both Figures 12 and 13 clearly confirm this result. Also, notice how rapidly P_c approaches its maximum value with increasing θ. The story of the blind mouse from Section IV.C provides the physical interpretation for this behavior: all other parameters held constant, collision probability is least when going with the flow of particles (or steamrollers), and is greatest when moving against them.

The variation of P_c with γ is a little more complicated. The partial derivative of P_c with respect to γ is

$$\frac{\partial P_c}{\partial \gamma} = \left[\tau\sec\gamma\tan\gamma\left(1-2\left(\frac{v_p}{v_m}\right)\sin\gamma\cos\theta+\left(\frac{v_p}{v_m}\right)^2\right)^{1/2} - \tau\left(\frac{v_p}{v_m}\right)\cos\theta\left(1-2\left(\frac{v_p}{v_m}\right)\sin\gamma\cos\theta+\left(\frac{v_p}{v_m}\right)^2\right)^{-1/2}\right] \exp\left\{\frac{-\tau}{|\cos\gamma|}\sqrt{1-2\left(\frac{v_p}{v_m}\right)\sin\gamma\cos\theta+\left(\frac{v_p}{v_m}\right)^2}\right\} . \quad \text{(IV.6)}$$

From equation (IV.6), the condition for minimum P_c, when all variables except γ are held constant, is

$$\frac{\sec\gamma\tan\gamma}{1+2\tan^2\gamma} = \frac{(\frac{v_p}{v_m})\cos\theta}{1+(\frac{v_p}{v_m})^2} \quad . \qquad \text{(IV.7)}$$

This imposing expression has a simple physical meaning:

(1) if v_p/v_m is less than one, P_c is minimized when the magnitude of the component of $\vec{v}_m$ in the direction of $\vec{v}_p$ is equal to v_p.

(2) if v_p/v_m is greater than one, P_c is minimized when the magnitude of the component of $\vec{v}_p$ in the direction of $\vec{v}_m$ is equal to v_m.

Once again, the blind mouse analogy may be helpful in understanding this behavior.

Before leaving this section, a few words are in order to clarify possible concern over the point of "undefined" collision probability shown in Figure 12. This anomaly only occurs when v_p/v_m is equal to one. For this particular speed ratio, when θ is zero, and γ is $\pi/2$, then the molecule is moving in concert with the ring particles. Thus, if it is not initially in contact with a particle, it never will be. On the other hand, if initially in contact with a particle, it will never separate from that particle. Therefore, the notion of a collision probability is meaningless under this unique circumstance.

V. DISCUSSION

A. GENERAL COMMENTS

To effectively exploit the collision theory developed in this paper, one generally must couple it with a ballistic transport model which provides values for the speed ratio, orbital inclination, and orbital azimuth. More accurate estimation of atmospheric density will result, although improvements in this area are limited by the lack of knowledge of details of a molecule-particle collision (i.e., the sticking coefficient described in Section I). The frequency of collisions also affects the spatial extent of the ring atmosphere. The trajectory of a molecule is initially determined by the nature of the production process, while its evolution is dictated by collisions.

Consideration of the special case of low energy, isotropic production processes (e.g., sublimation) allows one to apply the collision theory in making inferences on the spatial extent of the ring atmosphere.

B. APPLICATION TO AN ISOTROPIC, LOW ENERGY PRODUCTION PROCESS

Define an isotropic, low energy production process to be a mechanism which ejects molecules from ring particles such that:

(1) the direction of ejection relative to the particle is random.

(2) $v_{ej} << v_p$, which implies $v_p/v_m \cong 1$.

The orbit of a molecule, prior to collisions with ring particles, will be very nearly circular with a radius equal to that of its parent ring particle. The orbital plane will be only slightly inclined with respect to the ring plane, e.g., for sublimation the orbital plane is inclined at most 1° (see Section IV.A).

When a collision does occur, two outcomes are possible: the molecule "sticks," thus removing it from the atmosphere; or the molecule rebounds, assuming a new trajectory. In the latter case, what can be said about the new orbit? Since the collision will surely be inelastic to some degree, the speed of the rebounding particle relative to the ring particle is less than its incident speed. The speed ratio remains almost equal to one, implying a circular orbit. Following the approach used in Section IV.A, especially Figure 10, the primary effect of the inelastic collision is to reduce the inclination of the orbital plane. Thus, collisions act to reduce the spatial extent of the ring atmosphere; the details of this reduction being determined by the frequency of collisions, and the actual inelasticity of an individual collision.

The more frequent collisions are, the more closely confined to the vicinity of the ring will be the ring atmosphere. The collision theory can be used to examine collision frequency. Specifically, the average probability, as a function

of time, that a molecule has not suffered at least one collision is calculated below.

When a molecule is initially ejected, it may collide with a ring particle before ever leaving the ring plane. To calculate the probability that it collides with at least one ring particle, adopt a frame of reference in which the particles are fixed. The probability that the molecule is ejected from a particle in dz' is (see Figure 14)

$$P(z')dz' = \frac{1}{h} dz' , \quad 0 \leq z' \leq h , \tag{V.1}$$

while the probability that it is ejected into solid angle $d\Omega$ is

$$P(\Omega)d\Omega = \frac{1}{2} \sin\gamma' \, d\gamma' , \quad 0 \leq \gamma' \leq \pi , \tag{V.2}$$

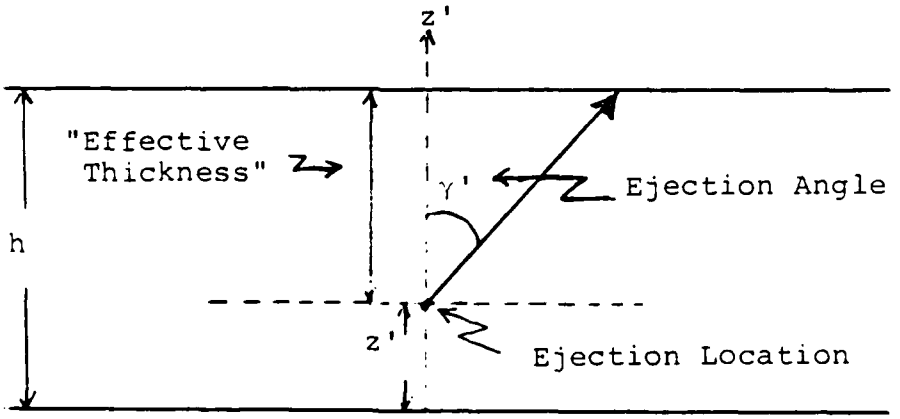

Figure 14. Ejection of a Molecule from a Particle at z'

since the production process is isotropic. The probability density for a molecule ejected at γ' from z' colliding with a ring particle before leaving the ring

$$P_c(\gamma',z') = \begin{cases} 1 - \exp\{\frac{-\tau(h-z')}{h\cos\gamma'}\} , & 0 \leq \gamma' < \frac{\pi}{2} \\ 1 - \exp\{\frac{+\tau-z'}{h\cos\gamma'}\} , & \frac{\pi}{2} \leq \gamma' \leq \pi \end{cases} \qquad (V.3)$$

which follows directly from equation (III.12), when the effective slab thickness is taken into account. The average probability of at least one collision for a molecule produced by an isotropic process is found by integrating over the product of equations (V.1), (V.2), and (V.3):

$$\bar{P}_c = \int_0^{\frac{1}{2}\pi} \int_0^h \frac{1}{2} h \sin\gamma' [1-\exp\{\frac{-\tau(h-z')}{h\cos\gamma'}]dz'd\gamma'$$

$$+ \int_{\frac{1}{2}\pi}^{\pi} \int_0^h \frac{1}{2} h \sin\gamma' [1-\exp\{\frac{+\tau z'}{h\cos\gamma'},\}]dz'\, d\gamma' .$$

Making a change of variables, $x = \cos\gamma'$ and $x = -\cos\gamma'$ in the first and second integrals, respectively, then integrating, yields

$$\bar{P}_c = 1 - \frac{1}{\tau}\int_0^1 x(1 - e^{-\tau/x})dx \qquad (V.4)$$

Therefore, the average probability that a molecule initially (i.e., t = 0) escapes the ring without collision is

$$\bar{P}_{esc} = 1 - \bar{P}_c = \frac{1}{\tau} \int_0^1 x(1 - e^{-\tau/x})dx \qquad (V.5)$$

Table 2 gives $\bar{P}_{ecs}$ for values of τ of interest for the rings. Notice that there is a significant chance of collision immediately after a molecule is ejected; suggesting that the spatial extent of the atmosphere is biased toward being closely confined to the ring even before subsequent evolution of the system is considered.

TABLE 2

AVERAGE PROBABILITY THAT A MOLECULE INITIALLY (t = 0) ESCAPES THE RING PLANE WITHOUT COLLIDING WITH RING PARTICLES

τ	$\bar{P}_{esc}$
0.1	0.837
0.5	0.556
1.0	0.390
1.5	0.296
2.0	0.235

During each orbital period, a molecule in a circular orbit traverses the ring two times. If that molecule has not collided with a ring particle, γ' retains its initial

value for each subsequent passage of the rings, and the probability that it does not collide with a ring particle during each period is $\exp\{\frac{-2\tau}{|\cos\gamma'|}\}$.[14] The probability that the molecule is ejected into solid angle $d\Omega$ <u>without</u> colliding with a ring particle is:

$$\frac{1}{2}\sin\gamma'\left[\int_0^h \frac{1}{h}(1-P_c(\gamma',z'))dz'\right]d\gamma' = \frac{1}{2}\sin\gamma'\left\{\begin{array}{l} \frac{\cos\gamma'}{\tau}(1-\exp\{\frac{-\tau}{\cos\gamma'}\}),\ 0 \le \gamma' < \frac{1}{2}\pi \\ \\ \frac{-\cos\gamma'}{\tau}(1-\exp\{\frac{\tau}{\cos\gamma'}\}),\ \frac{1}{2}\pi \le \gamma' \le \pi \end{array}\right\} d\gamma' ,$$

If T_p is the number of completed orbital periods, then the probability that the molecule has not collided with any particle as a function of time, given in terms of T_p, is

$$\bar{P}_{esc}(T_p) = \int_0^{\pi} \frac{1}{2}\sin\gamma'\left\{\begin{array}{l} \frac{\cos\gamma'}{\tau}(1-\exp\{\frac{-\tau}{\cos\gamma'}\},\ 0 \le \gamma' < \frac{1}{2}\pi \\ \\ \frac{-\cos\gamma'}{\tau}(1-\exp\{\frac{\tau}{\cos\gamma'}\},\ \frac{1}{2}\pi \le \gamma' \le \pi \end{array}\right\} \exp\left(\frac{-2\tau T_p}{|\cos\gamma'|}\right) d\gamma' ,$$

or

$$\bar{P}_{esc}(T_p) = \frac{1}{\tau}\int_0^1 x e^{-2\tau T_p/x}(1-e^{-\tau/x})dx . \qquad (V.6)$$

---

[14] This result can be easily understood by considering a slab of thickness 2h. Extending this reasoning, if T_p periods have been completed, the probability of no collision for a molecule initially escaping is $\exp\{-2\tau T_p/|\cos\gamma'|\}$.

Table 3 gives the probability that a molecule has remained free of collisions, as a function of time (given in orbital periods) for various optical thicknesses. These results

TABLE 3

VARIATION OF $\bar{P}_{esc}$ WITH τ AND T_p

$\bar{P}_{esc}$

T_p	$\tau = 0.1$	$\tau = 0.5$	$\tau = 1.0$	$\tau = 1.5$	$\tau = 2.0$
0	0.837	0.556	0.390	0.296	0.235
1	0.519	0.106	0.021	0.005	0.001
2	0.357	0.028	0.002	1.56×10^{-4}	~0
3	0.255	0.008	1.94×10^{-4}	~0	~0
4	0.186	0.002	~0	~0	~0
5	0.138	0.001	~0	~0	~0

strongly imply collisions are quite frequent for isotropic, low energy production processes. This in turn implies that the ring atmosphere associated with this process will tend to be more concentrated in the vicinity of the ring than analysis of the distribution of particles prior to collision would indicate.

C. ON MULTIPLE COLLISIONS

The collision probability theory developed in this thesis cannot be used to precisely calculate the probability of

multiple collisions, i.e., the chance that a molecule collides with two, three, etc., particles during a single passage through the rings. Computer-simulation models may provide the best way to approach this problem.

Based on the results of the preceding section, the probability of at least one collision is quite high in the A and B rings. This suggests that multiple collisions could be a significant factor in analysis of the ring atmosphere.

VI. CONCLUSIONS

In this paper, a model for collisions between ring particles and molecules in the ring atmosphere has been developed. The resulting expressions for the probability of at least one collision when a molecule passes through the ring are

$$P_c = 1 - \exp\{\frac{-\tau}{|\cos \gamma'|}\} , \qquad \text{(III.12)}$$

for a frame of reference where the ring particles are fixed, and

$$P_c = 1-\exp\{\frac{-\tau}{|\cos \gamma|}\sqrt{1-2(\frac{v_p}{v_m}) \sin\gamma \cos\theta + (\frac{v_p}{v_m})^2}\} , \qquad \text{(IV.1)}$$

for a frame of reference fixed on Saturn in which the particles are seen to orbit the planet. They are more complete than those currently employed in analysis of the ring atmosphere, since specifics on molecular trajectory and the relative velocity of a molecule with respect to the ring particles are included. Thus, this analytic collision theory is compatible with computer-simulated ballistic transport models, since they include similar effects.

The frequency of collisions influences both the total population of molecules in the ring atmosphere, and their

spatial distribution, as shown by Dennefeld (1974). Since knowledge of molecular sources is still evolving, and understanding of the dynamics of an individual collision (e.g., Dennefeld's "sticking coefficient") is in its infancy, improved estimates of molecular populations cannot be made based on this revision of collision theory, alone. Inferences on spatial distribution can, however, be made. When a low energy, isotropic production process is considered for optical thicknesses characteristic of the A and B rings of Saturn, collisions are found to be quite frequent. This implies an atmosphere closely confined to the vicinity of the rings. Extending this result to more energetic production processes (e.g., see Section III.A) implies that the ring atmosphere will be toroidal in shape. Thus, assuming a toroidal shape will probably be more productive than assuming spherical shape in future studies of the ring atmosphere.

As a final note, the collision theory used here in connection with the ring atmosphere should be useful in another related application. Ballistic transport of macroscopic particles produced during meteroid impacts may account for some of the radial structure in Saturn's rings (Ip, 1983; Durisen, 1984). These particles form a "chip halo" in the vicinity of the rings. As long as the chips are small relative to ring particles, the model developed here applies for calculation of collision probabilities.

APPENDIX A

RING NOMENCLATURE AND DIMENSIONS

Saturn's ring system consists of seven distinct rings. The A, B, C, D, and F rings are characterized by distinct boundaries. Their nominal thicknesses are not more than ~200 m (Cuzzi et al., 1984), and may well be less than 5-10 m (Bridges et al., 1984). The E and G rings are diffuse structures with poorly defined boundaries and nominal thicknesses of ~10^3 and 10^2 km, respectively (Cuzzi et al., 1984). Table A1 is a summary of the radial structure of the ring system. Note that the F and G rings are quite narrow.

TABLE A1

RADIAL STRUCTURE OF SATURN'S RINGS

	Boundaries		
Ring/Region	R_s	km	mass
D	~1.11-1.235	66,970-74,510	?
C	1.235-1.525	74,510-92,000	2×10^{-9} Ms
B	1.525-1.949	92,000-117,580	5×10^{-8} Ms
Cassini Division	1.949-2.025	117,580-122,170	1×10^{-9} Ms
A	2.025-2.267	122,170-136,780	1×10^{-8} Ms
F	2.324	140,180	?
G	2.82	170,100	1×10^{-17} Ms
E	3-8	181,000-438,000	?

R_s = 60,330 km (Saturn's radius) $M_s = 5.685 \times 10^{26}$ kg (Saturn's mass)

The Cassini Division is a well-defined gap between the A and B rings, which is by no means "empty."

The optical depth, τ, is a dimensionless parameter directly related to mass density. Table A2 gives average optical thickness for the main rings. Optical thickness in the other rings is much lower. Since optical thickness increases with increasing mass density, it follows that the A and B rings should be the most significant sources of a ring atmosphere.

TABLE A2

AVERAGE OPTICAL THICKNESS OF THE MAIN RINGS BASED ON STELLAR OCCULTATION OBSERVATIONS FROM VOYAGER 2 (ESPOSITO ET AL., 1984)

REGION	BOUNDARIES (R_S)	τ_{AVE}
inner C	1.24-1.39	0.08
outer C	1.39-1.52	0.15
inner B	1.52-1.66	1.21
middle B	1.66-1.72	1.76
outer B	1.72-1.95	1.84
Cassini Division	1.95-2.02	0.12
inner A	2.02-2.16	0.70
outer A	2.16-2.27	0.57

R_S = 60,330 km

APPENDIX B

DERIVATION OF P_c WHEN v_p IS NOT EQUAL TO ZERO

In Section II of the main body of this paper, an expression for the probability that a molecule passing through a ring collides with at least one ring particle, P_c, was derived in a frame of reference in which the ring particles are fixed (i.e., v_p equal to zero). Here it will be demonstrated that the same expression for P_c results when the derivation is made in a frame of reference where the slab translates with $\vec{v}_p$ not equal to zero.

The model upon which this derivation is based is the same as that described in Section II. Reviewing, a molecule passes through a region in space which contains randomly distributed (spatially) spherical particles. This region, the "slab," is of large extent, L, in two dimensions- and of relatively small thickness, h. The entire slab moves through space with constant velocity, $\vec{v}_p$, in a direction normal to the slab's thickness ($\vec{v}_p$ is measured relative to some inertial frame of reference). The radius, or "size," of each particle is restricted to an interval $[r_{min}, r_{max}]$ with r_{min} much greater than the nominal radius of the molecule, and with r_{max} much smaller than h. The size distribution of the particles may be either discrete or continuous. The number of particles in the slab is further assumed to be large.

Finally, the number density as a function of size is denoted by n(r), defined as the number of particles:

(1) of radius r per unit volume (discrete size distributions).

(2) in the radius interval [r,r+dr] per unit volume (continuous size distributions).

What is the probability that the molecule collides with a particle in the slab? In Section II this question is answered with relative ease by converting to a frame of reference in which the particles are at rest. Below, no such simplification is made.

When $\vec{v}_p$ is not equal to zero, the notion of cylindrical "collision regions," used in Section II, loses its validity. Another approach must be taken. Suppose that the slab is subdivided into regions of very small thickness, Δh, and finite area L^2 (see Figure B1). If the probability that the

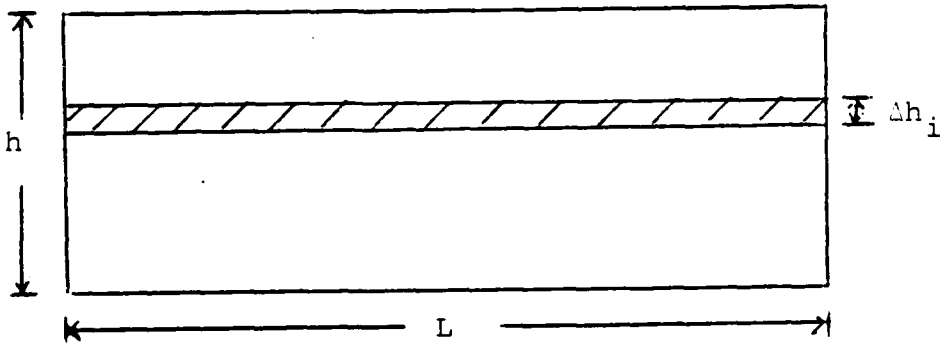

Figure B1. Edgeview of the Slab and a Representative Subregion

molecule does not collide with particles of size r whose centers lie in a specific sublayer can be calculated (call this $P_{no}(r,\Delta h_i)$), then the total probability of no collision with particles of size r will be

$$P_{no}(r) = \prod_i P_{no}(r,\Delta h_i) , \qquad (B.1)$$

since all of the small sublayers are mutually independent.[15] The collision probability, following Section II, is

$$P_c = 1 - \prod_j P_{no}(r_j) = 1 - \prod_j \prod_i P_{no}(r_j,\Delta h_i) \qquad (B.2)$$

for discretely distributed r.

The problem now is to find an expression for $P_{no}(r_j,\Delta h_i)$. First, the case of discrete r is solved from which the continuous solution can be deduced. Adopt a point of view in which the molecule has radius r, and the particles are point masses (on reflection this is analogous to the real situation as far as collision probabilities are concerned). Then, $P_{no}(r_i,\Delta h_i)$ can clearly be seen to be equivalent to the probability that the volume in the subslab "swept out" by

---

[15] Two observations on equation (B.1) are in order. First, there are infinitely many factors in the product over i. Second, $P_{no}(r,\Delta h_i)$ must be the same for all i, since in this model the statistical properties of each subregion are identical. Equation (B.1) may be difficult to interpret at this point, but its meaning will be clarified later in this appendix.

the passing molecule has no particles centered within it. The probability of no collisions with particles of size r_j in subslab Δh_i is:

$$P_{no}(r_j,\Delta h_i) = \left[\frac{L^2\Delta h_i - (\text{Vol. Swept Out})\, n(r_j) L^2 \Delta h_i}{L^2 \Delta h_i}\right] , \qquad (B.3)$$

since the particles are assumed to be randomly distributed throughout the slab (see Section II for a more detailed explanation of this assertion). In general, the mathematics involved in finding this "volume swept out" is extremely tedious. To demonstrate the method, the special case of γ equal to zero or π (molecular path normal to the plane of the slab) is solved below.

On what portion of its path can a molecule potentially collide with a ring particle of size r_j in Δh_i? Consideration of Figure B2 shows that the pertinent part of the path is of length $2r_j$. If time, t, is set equal to zero when the molecule initially encounters the subslab (Figure B2(a)), then at any t such that

$$0 \leq t \leq \frac{2r_j}{v_m} ,$$

the molecule will collide with any particle is a disk of radius (call this the "interaction radius")

$$R_I(t) = (2rv_m t - v_m^2 t^2)^{1/2} , \qquad (B.4)$$

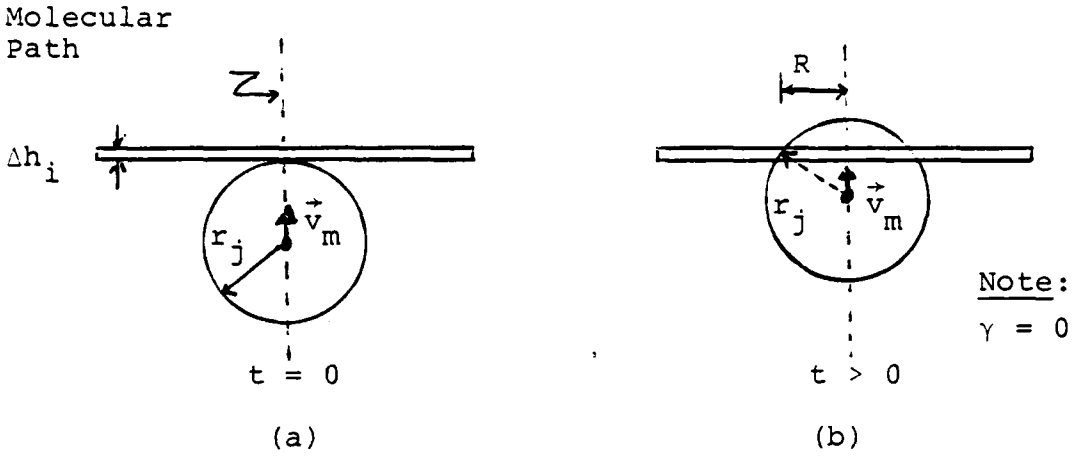

Figure B2. Relationship Between the Molecule and a Subslab When Collision with Ring Particles Centered in the Subslab is: (a) First Possible (t = 0); (b) At Any Time, t, Such That $0 < t < 2r_j/v_m$

where R_I is defined as shown in Figure B2(b). As the interaction radius evolves, the particles in the subslab move with speed v_p. Considering these two factors together, it can be deduced that an oblong "interaction region" in the subslab must be particle-free, if no collisions are to occur. To actually calculate this volume, first relate R_I to the distance that the slab moves in time t, call this D_I; clearly

$$D_I(t) = v_p t \ . \tag{B.5}$$

Substituting from equation (B.5) into equation (B.4) yields

$$R_I(D_I) = \left(2r\left(\frac{v_m}{v_p}\right)D_I - \left(\frac{v_m}{v_p}\right)^2 D_I^2\right)^{1/2} \tag{B.6}$$

Figure B3 is a sketch of equation (B.6). The oblong area in Figure B3 (bounded by the graph for R_I and its reflection across the D_I-axis, which is shown by a dashed line) cannot

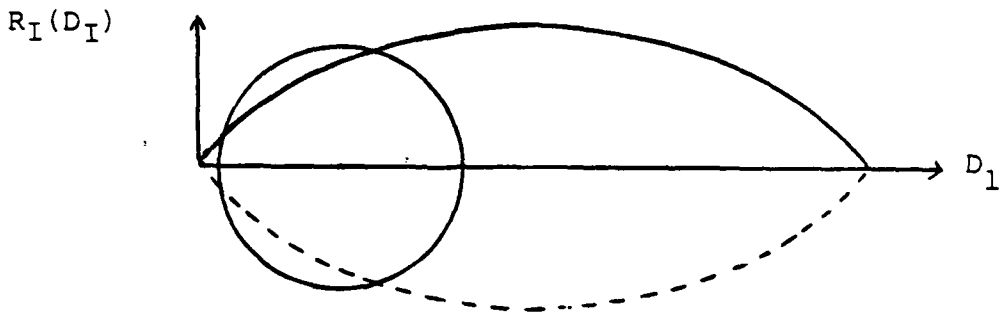

Figure B3. R_I as a Function of D_I

represent the projection of the interaction region into the plane of the subslab. Consideration of instantaneous interaction region, represented by the circle in Figure B3, illustrates that the actual interaction region is larger. Knowing $R_I(D_I)$, the function enveloping the interaction region can be found. Call this function R_I^*.

Consider Figure B4; it shows one-quarter of the interaction volume's projection into the plane of Δh_i. At a given time t', D_I' equals $v_m t'$, and the interaction radius is R_I'. The value of $R''(D_I)$ for any D_I is

$$R_I''(D_I') = \begin{cases} ([R_I(D_I)[^2-[D_I'-D_I]^2)^{1/2}]; & |D_I-D_I'| < R_I'(D_I') \\ 0 & ; \text{ otherwise} \end{cases} . \quad (B.7)$$

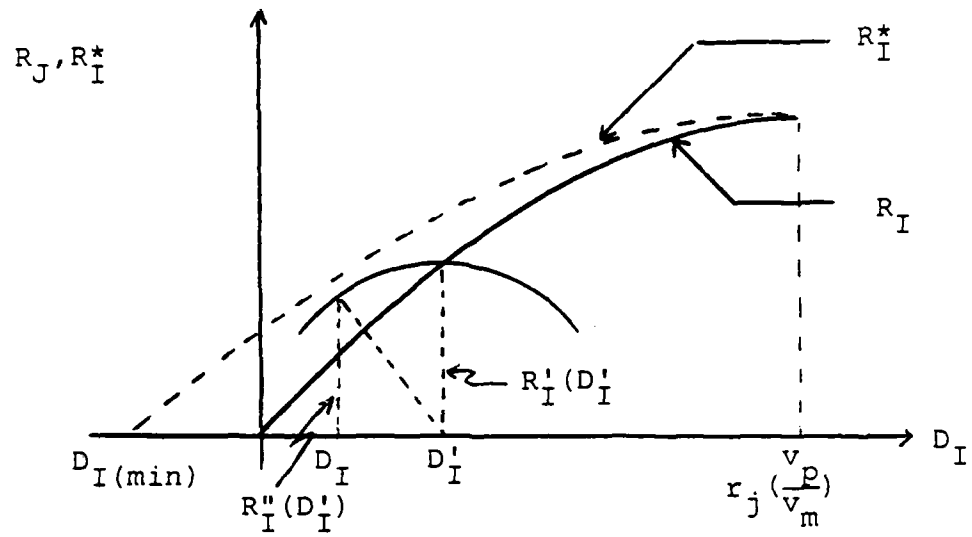

Figure B4. Geometry for Calculating R_I^*

$R_I^*(D_I)$ is the maximum value of $R_I''(D_I')$. Setting the first derivative of R_I'' with respect to D_I' equal to zero, and solving for D_I' gives

$$D_I' = \frac{D_I + r_j(\frac{v_m}{v_p})}{[1 + (\frac{v_m}{v_p})^2]}, \tag{B.8}$$

when equation (B.6) is substituted into equation (B.7). Substituting from equation (B.8) into equation (B.7) gives the maximum value of $R_I''(D_I')$ for a given D_I, i.e.,

$$R_I^*(D_I) = [(\frac{v_m}{v_p})\{\frac{r_j^2(\frac{v_m}{v_p}) + 2r_j D_I - D_I^2(\frac{v_m}{v_p})}{1 + (\frac{v_m}{v_p})^2}\}]^{1/2}. \tag{B.9}$$

Using equation (B.9), the region in the sublayer that must be devoid of particles of size r_j if no collision is to occur between the molecule and such particles, has

$$\text{Volume} = (\Delta h_i)\, 4 \int_{D_{I(min)}}^{r_j (\frac{v_p}{v_m})} R^*(D_I)\, dD_I \,, \tag{B.10}$$

where

$$D_{I(min)} = [(\frac{v_p}{v_m}) - \{1 + (\frac{v_p}{v_m})^2\}^{1/2}]\, r_j \,. \tag{B.11}$$

When the integral in equation (B.10) is evaluated,

$$\text{Volume} = \pi r_j^2 \{1 + (\frac{v_p}{v_m})^2\}^{1/2} \Delta h_i \,, \tag{B.12}$$

and substituting into equation (B.3) gives

$$P_{no}(r_j, \Delta h_i) = [\frac{L^2 \Delta h_i - \pi r_j^2 \{1+(\frac{v_p}{v_m})^2\}^{1/2} \Delta h_i \; n(r_j) L^2 \Delta h_i}{L^2 \Delta h_i}] \,. \tag{B.13a}$$

Equation (B.13) can be rewritten as

$$P_{no}(r_j, \Delta h_i) = [1 - \frac{\pi r_j^2 n(r_j) \{1 + (\frac{v_p}{v_m})^2\}^{1/2}}{L^2 n(r_j)}]^{n(r_j) L^2 \Delta h_i} \,. \tag{B.13b}$$

Summing over i yields the probability that no collision occurs in the entire salb, i.e.,

$$P_{no}(r_j) = \left[1 - \frac{\pi r_j^2 n(r_j)\{1 + (\frac{v_p}{v_m})^2\}^{1/2}}{L^2 n(r_j)}\right]^{n(r_j)L^2h} \qquad \text{(B.14a)}$$

Multiplying the second term in the brackets in equation (B.14) by h/h yields

$$P_{no}(r_j) = \left[1 - \frac{\pi r_j^2 n(r_j)\{1 + (\frac{v_p}{v_m})^2\}^{1/2} h}{L^2 n(r_j) h}\right]^{n(r_j)L^2h} \qquad \text{(B.14b)}$$

but the total number of particles of size r_j, $n(r_j)L^2h$, is assumed to be large, so equation (B.14b) can be rewritten in exponential form as

$$P_{no}(r_j) = \exp\{-\pi r_j^2 n(r_j)\{1 + (\frac{v_p}{v_m})^2\}^{1/2} h\} \qquad \text{(B.14c)}$$

Therefore, the collision probability is (from equation (B.2))

$$P_c = 1 - \prod_j \exp\{-\pi r_j^2 n(r_j)\{1 + (\frac{v_p}{v_m})^2\}^{1/2} h\} ,$$

$$P_c = 1 - \exp\{-\pi(\sum_j r_j^2 n(r_j))\{1 + (\frac{v_p}{v_m})^2\}^{1/2} h\} , \qquad \text{(B.15a)}$$

for r_j discrete, or by extension

$$P_c = 1 - \exp\{-\pi(\int r^2 n(r)dr)\{1 + (\frac{v_p}{v_m})^2\}^{1/2} h\} , \qquad \text{(B.15b)}$$

for continuous r.

Comparison of equations (B.15a) and (B.15b) with equations (II.7) and (II.8) (with γ equal to zero), reveals the equivalence of solving the collision probability problem in two different frames-of-reference. That the results are the same is not surprising. What is interesting is the relative difficulty of the two approaches.

APPENDIX C

FRAME OF REFERENCE CONVERSION

In Section II of this thesis, the collision probability, P_c, is calculated in a frame of reference in which the ring particle velocity, $\vec{v}_p$, is equal to zero. When coupling the collision theory with ballistic transport models, a more convenient frame of reference is a localized cartesian system fixed in the vicinity of the intersection of the molecule's path and the ring. The x-axis is in the direction of motion of the ring particles; the y-axis is directed radially outward from Saturn; and the z-axis is normal to the ring plance (see Figure C1). Here the direction cosines of α, β,

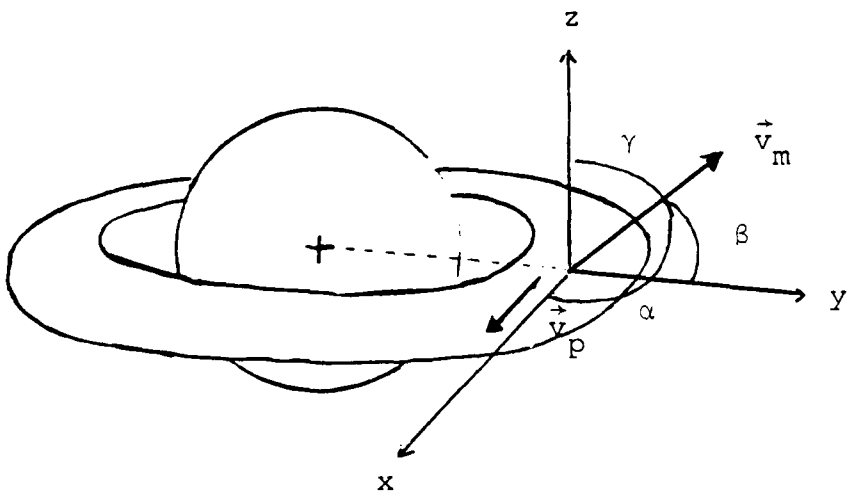

Figure C1. A Coordinate System Fixed at a Specific Location in the Rings

and γ quite accurately describe the path of the molecule through the ring which is essentially linear owing to the great radius of curvature of the molecular trajectory ($\sim 10^{5}$ km) relative to the extreme thinness ($\sim 10^{-1}$ km) of the rings.

Let the frame of reference, for which the ring particles in the region through which the molecule passes are at rest, be called the "primed" system. The simplest coordinate system that can be used to describe the molecule's path in this frame of reference will have the x'-, y'-, and z'-axes in the same direction as the corresponding axes in the un-primed system with the y'-axis in the direction of $\vec{v}_p$ (see Figure C2). α', β', and γ' yield direction cosines describing the molecules path in the primed system.

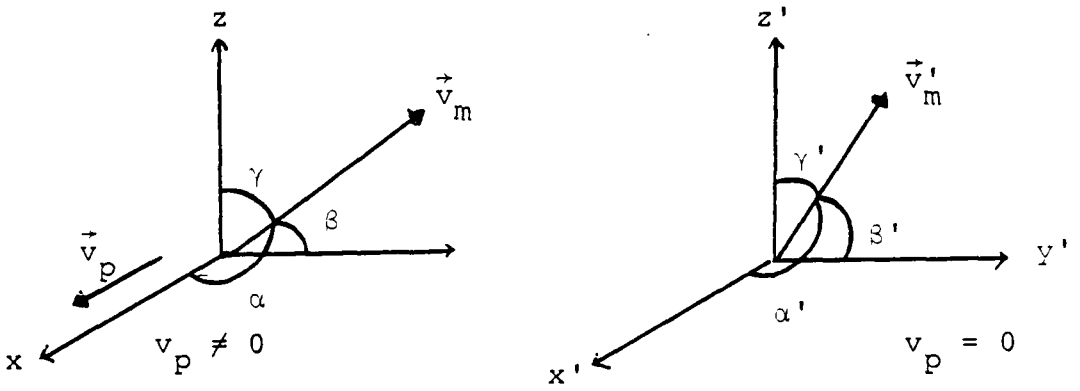

Figure C2. Direction Cosines in the Two Coordinate Systems

In Section II the collision problem is attacked using the primed system. The expressions for P_c derived there

(equations (II.5) and (II.6)) contain a factor of $\cos \gamma'^{-1}$. An expression for this factor in terms of α, β, γ, v_m, and v_p must be found to represent P_c in the unprimed system. First, note that:

$$\vec{v}'_m = \vec{v}_m - \vec{v}_p \qquad \text{(C.1)}$$

gives the relationship between the molecular velocities in the two systems. Writing vector equation (C.1) in component form yields:

$$v'_{mx} = v_{mx} - v_p \; ; \qquad \text{(C.2a)}$$

$$v'_{my} = v_{my} \; ; \qquad \text{(C.2b)}$$

$$v'_{mz} = v_{mz} \; . \qquad \text{(C.2c)}$$

keeping in mind the definitions of the two systems given in Figure C1. Equations (C.2) can be rewritten in terms of the direction cosines:

$$v'_m \cos \alpha' = v_m \cos \alpha - v_p \; ; \qquad \text{(C.3a)}$$

$$v'_m \cos \beta' = v_m \cos \beta \; ; \qquad \text{(C.3b)}$$

$$v'_m \cos \gamma' = v_m \cos \gamma \; . \qquad \text{(C.3c)}$$

Squaring equations (C.3) and adding yields:

$$v_m'^2(\cos^2\alpha' + \cos^2\beta' + \cos^2\gamma') = v_m^2(\cos^2\alpha + \cos^2\beta + \cos^2\gamma) + v_p^2 - 2v_m v_p \cos\alpha \ . \qquad (C.4)$$

Since the sum of the squares of direction cosines is identically equal to one, equation (C.4) becomes

$$v_m'^2 = v_m^2 + v_p^2 - 2\, v_m v_p \cos\alpha \ . \qquad (C.5)$$

From equation (C.3c)

$$v_m' = v_m\left(\frac{\cos\gamma}{\cos\gamma'}\right) \ , \qquad (C.6)$$

which, when substituted into equation (C.5), yields

$$v_m^2\left(\frac{\cos\gamma}{\cos\gamma'}\right)^2 = v_m^2 + v_p^2 - 2\, v_m v_p \cos\alpha \ . \qquad (C.7)$$

Solving for $|\cos\gamma'|^{-1}$ gives

$$\frac{1}{|\cos\gamma'|} = \frac{1}{|\cos\gamma|}\sqrt{1-2\left(\frac{v_p}{v_m}\right)\cos\alpha+\left(\frac{v_p}{v_m}\right)^2} \ . \qquad (C.8)$$

Equation (C.8) is the fundamental result of this derivation. When substituted into equations (II.5) and (II.6), the resulting expressions for P_c, equations (II.7) and (II.8), have

the advantage that they are written in terms of the frame of reference most often utilized when studying the rings.

APPENDIX D

RELATING ORBITAL AZIMUTH TO THE DIRECTION COSINES

Consider a unit vector, $\hat{u}$, as shown in Figure D1. Its direction can be specified by the direction cosines (α,β,γ), or by (γ,θ) where θ is called the "orbital azimuth." How are these two representations related?

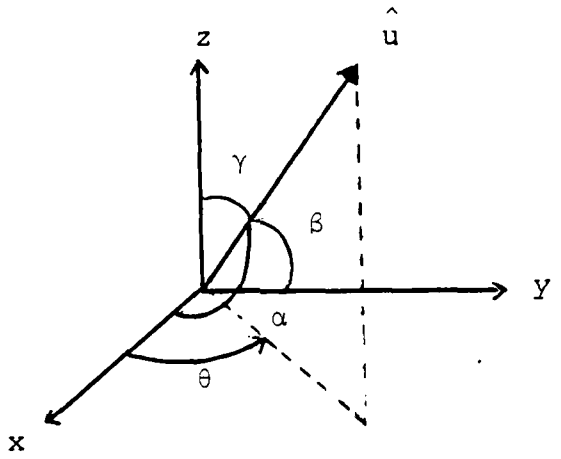

Figure D1. Angles Used to Specify the Direction of $\hat{u}$

First, note that

$$\cos^2\alpha + \cos^2\beta + \cos^2\gamma \equiv 1 ,$$

or

$$\cos^2\beta = 1 - \cos^2\alpha - \cos^2\gamma . \qquad (D.1)$$

The x and y components of $\hat{u}$ are

$$u_x = \cos \alpha \ , \tag{D.2a}$$

$$u_y = \cos \beta \ . \tag{D.2b}$$

By definition

$$\tan \theta = \frac{u_y}{u_x} \ , \tag{D.3}$$

and substituting from equations (D.2) gives

$$\tan \theta = \frac{\cos \beta}{\cos \alpha} \ . \tag{D.4}$$

Squaring equation (D.4) and substituting from equation (D.1) yields

$$\tan^2\theta = \frac{1 - \cos^2\alpha - \cos^2\gamma}{\cos^2\alpha} \ . \tag{D.5}$$

Rearranging equation (D.5) gives

$$(1 + \tan^2\theta)\cos^2\alpha = 1 - \cos^2\gamma \ ,$$

but

$$1 + \tan^2\theta \equiv \sec^2\theta \quad \text{and} \quad 1 - \cos^2\gamma \equiv \sin^2\gamma \ ,$$

so

$$\sec^2\theta \cos^2\alpha = \sin^2\gamma \qquad (D.6)$$

Finally,

$$\cos \alpha = \sin \gamma \cos \theta \ , \qquad (D.7)$$

which is useful for expressing P_c in terms of γ and θ.

APPENDIX E

SOME RESULTS OF CALCULATION OF P_c

This appendix consists of several examples of results for the calculation of P_c, based on the equation

$$P_c = 1 - \exp\left\{\frac{-\tau}{|\cos\gamma|}\sqrt{1-2\left(\frac{v_p}{v_m}\right)\sin\gamma\cos\theta+\left(\frac{v_p}{v_m}\right)^2}\right\} .$$

Calculations were made over the range of optical thickness pertinent to Saturn's A and B rings:

$$0.1 \leq \tau \leq 2.0 .$$

The figures have been arranged to allow one to compare the effect of varying the parameters of the equation.

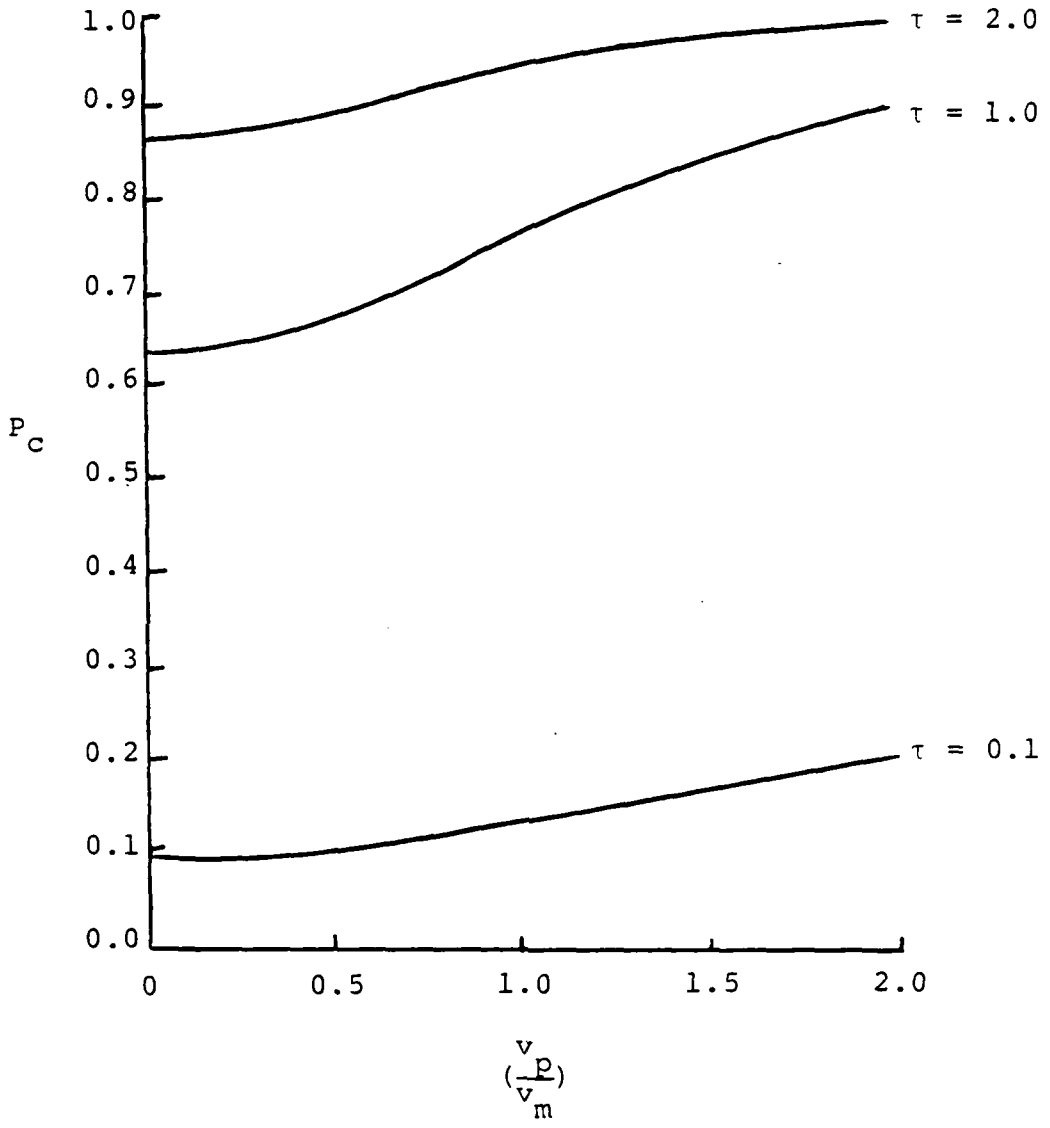

Figure E1. Collision Probability for $\gamma = 0$

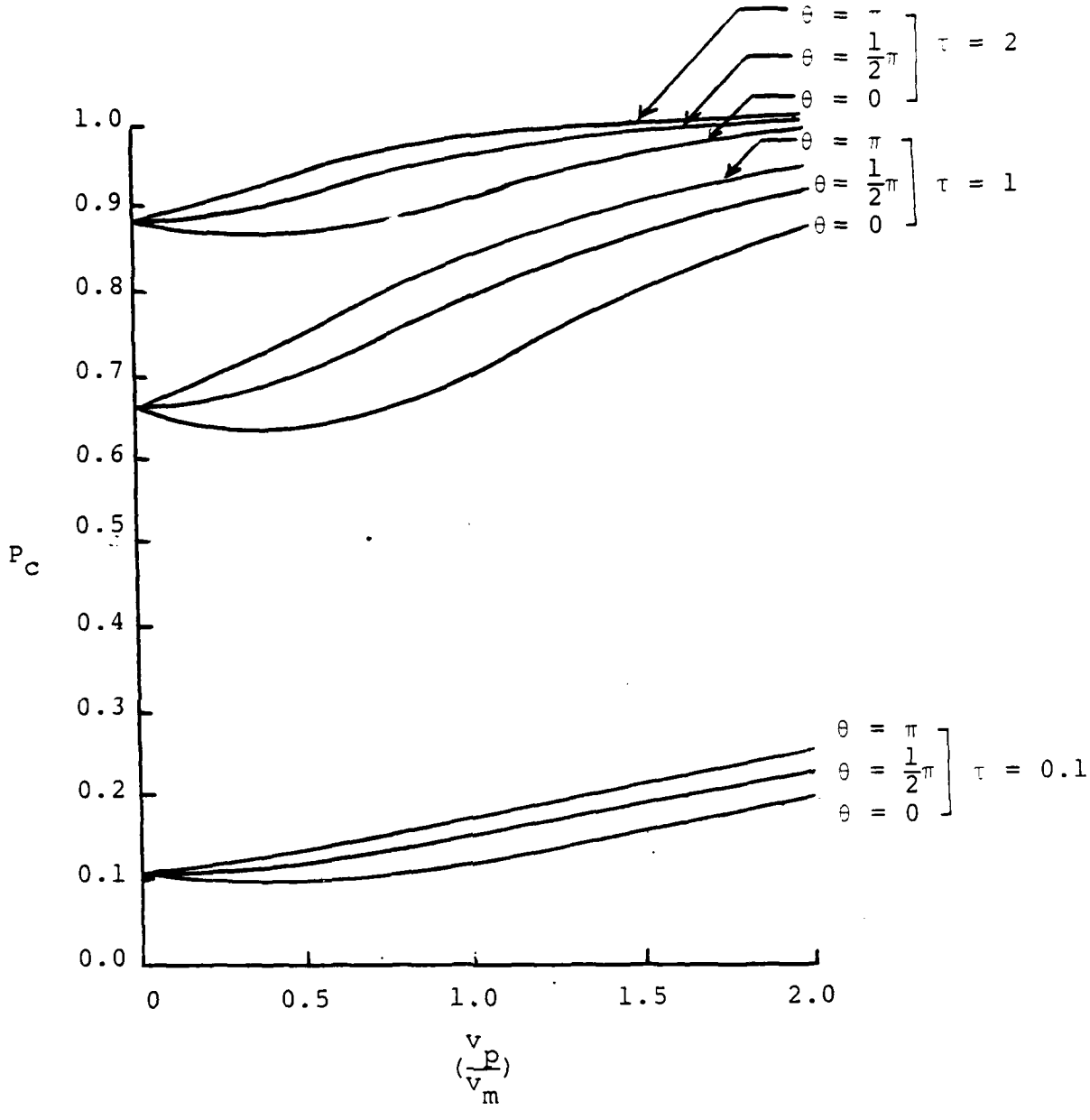

Figure E2. Collision Probability for $\gamma = \frac{1}{8}\pi$

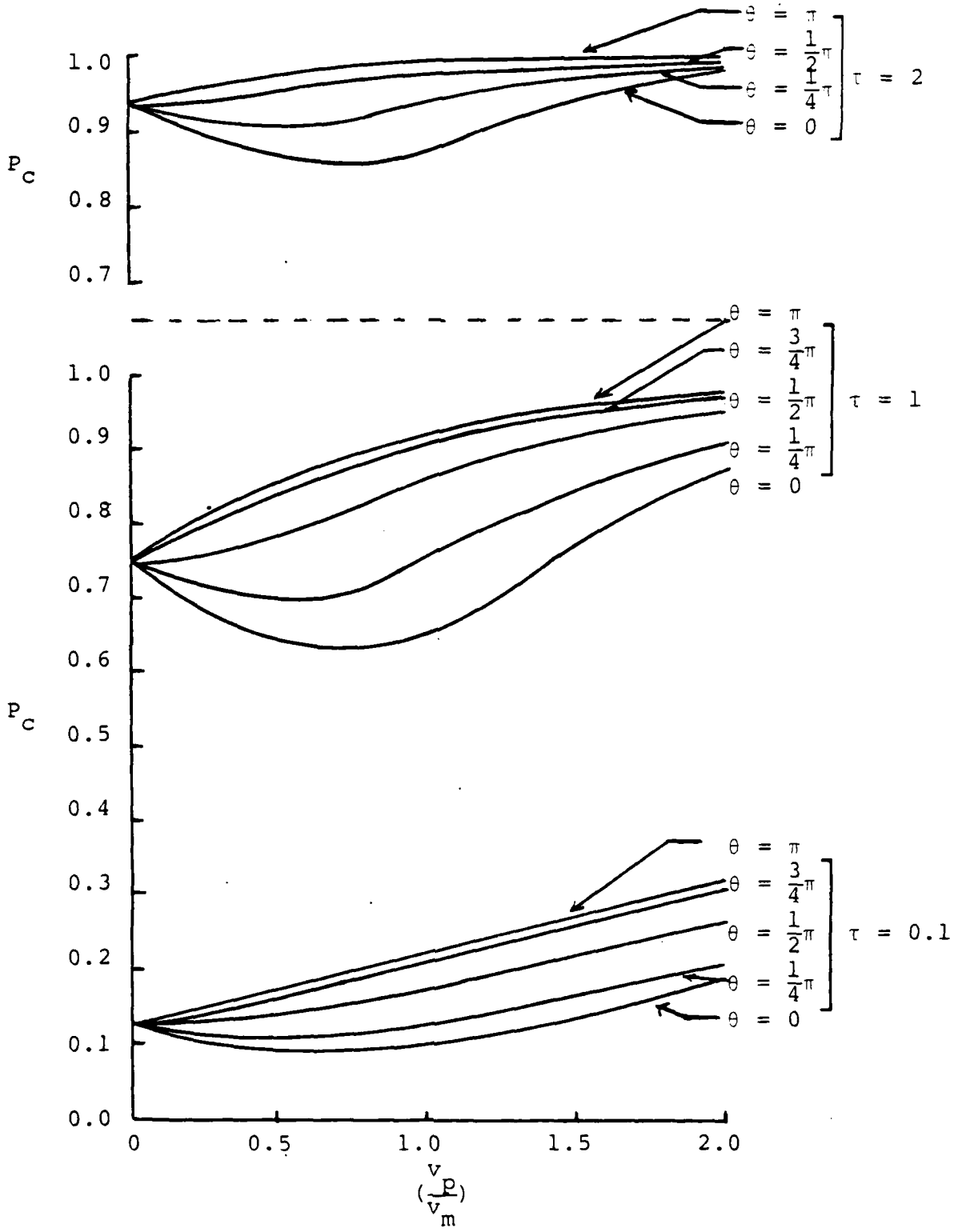

Figure E3. Collision Probability for $\gamma = \frac{1}{4}\pi$

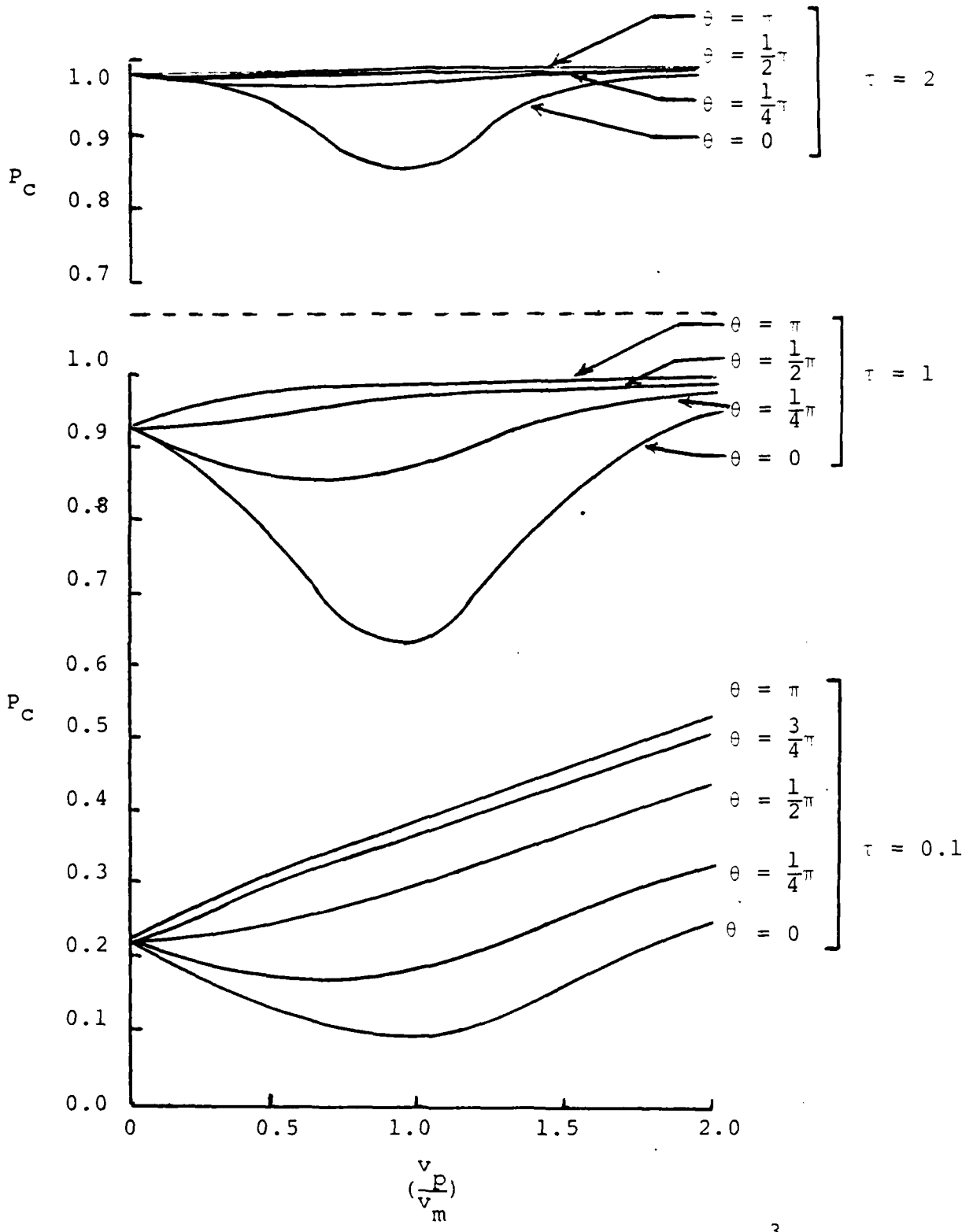

Figure E4. Collision Probability for $\gamma = \frac{3}{8}\pi$

APPENDIX F

ANNOTATED BIBLIOGRAPHY

The purpose of this appendix is to briefly review those papers which should be of particular interest to one who wishes to study ring atmospheres.

General Theory

1. Blamont, J. 1974. "The 'Atmosphere' of the Rings of Saturn," in NASA SP-343, edited by Palluconi and Pettengill, 125-129.

   Blamont's paper is the transcript of his comments, delivered at a planning conference for the Pioneer II mission. His theoretical model is not detailed but results for the H_2O, H, and OH atmospheres are given. Estimates of Lyman-α emissions are also presented.

2. Dennefeld, M. 1974. "Theoretical Studies of an Atmosphere around Saturn's Rings," in Exploration of the Planetary System, edited by Woszczyk and Iwaniszewska, 471-481.

   Dennefeld was Blamont's student. His paper predicts the density of the ring atmosphere (and that associated with Titan). The sources considered are sublimation, bombardment by meteoroids, solar and interstellar wind effects, and photodisssociation of H_2O on the ring particles. The resulting estimates are outdated for the most part, primarily because the production mechanisms are now betterunderstood. The conceptual model for calculation of atmospheric densities, however, is of enduring significance. It concisely gives a qualitative way to describe the atmosphere. One questionable assertion made in the paper is that the H atmosphere will be spherical due to collisions between the H atoms and ring particles; this is at odds with the results of the present thesis. Also, Dennefeld estimates the collision probability to be equal to the optical thickness.

Ballistic Transport Models

1. Durisen, R.H. 1984. "Transport Effects due to Particle Erosion Mechanisms," in Planetary Rings, edited by Greenberg and Brahic, 416-446. University of Arizona Press.

   Durisen presents a detailed model aimed primarily at prediction of "chip halo," i.e., macroscopic ejecta resulting from meteroid impact, formation (the model is in general applicable to the ring atmosphere, too). The assumption of "prompt absorption" (i.e., particle-molecule collisions are inelastic) is made for calculations in his paper. In calculating collision probability, Durisen accounts for "slant path" of a molecule through the rings, but it is not clear whether he considered the relative speed of the particles versus the molecule. The results of his studies indicate that transport of eroded material across the rings may be significant for understanding the fine structure observed in the rings.

2. Ip, W-H. 1983. "Collisional Interaction of Ring Particles: the Ballistic Transport Process," Icarus 54: 253-262.

   Ip develops a transport model independently of Durisen. The results of the two different approaches are quite compatible. Ip is able to assume partially elastic collisions, since he employs the Monte Carlo method in his simulation. He takes the collision probability to depend on optical thickness only; a more detailed estimate of P_c could easily be incorporated into his model, though.

Sources (Production Mechanisms)

1. Carlson, R.W. 1980. "Photosputtering of Ice and Hydrogen around Saturn's Rings," Nature 283: 461.

   Carlson argues that photodissociation of H_2O on ring particles could account for the relatively high population of H atoms actually measured in the vicinity of the A and B rings. Note that he calculates collision probability using $1-e^{-\tau}$ with τ equal to one. He takes the sticking coefficient to be 0.22, but this value is based on laboratory experiments (Brackmann and Fite, 1961) which do not closely match the conditions in Saturn's rings. The overall influence of the uncertainty in these two factors should not affect the order of magnitude of his calculations, but probably limits the

precision of his estimation of total production rate needed to produce the observed H atom population.

2. Cheng, A.F. and Lanzerotti, L.J. 1978. "Ice Sputtering by Radiation Belt Protons and the Rings of Saturn and Uranus," Journal of Geophysical Research 83: 2597-2602.

   This paper is a detailed summary of sputtering effects on ring particles.

3. Cheng, A.F., Lanzerotti, L.J., and Pironelle, V. 1982. "Charged Particle Sputtering of Ice Surfaces in Saturn's Magnetosphere," Journal of Geophysical Research 87: 4567-4570.

   Using information derived from the Pioneer II, Voyager I and Voyager II missions, the authors reconsider the sputtering mechanism, revising the result of their earlier (1978) paper. Since the actual ion fluxes observed were lower than those they assumed in 1978, the authors conclude that ion sputtering probably does not contribute significantly to the H atom atmosphere in the vicinity of the A and B rings of Saturn.

4. Ip, W-H. 1978. "On the Lyman-alpha Emission from the Vicinity of Saturn's Rings," Astronomy and Astrophysics 70: 435-437.

   This short paper suggests that H^+ ions escaping from Saturn's atmosphere may collide with ring particles where they are neutralized and re-emitted, thus contributing to the neutral H atmosphere in the vicinity of the rings.

5. Morfill, G.E. et al. 1983. "Some Consequences of Meteroid Impacts on Saturn's Rings," Icarus 55: 439-447.

   Morfill et al. make careful estimates of the meteroid flux in the vicinity of Saturn. Using this estimate, coupled with a model for analyzing the effects of meteroid impact on ring particles, they proceed to make predictions about the ring halo, plamsa production, and the ring atmosphere. The authors conclude that meteroid impacts should contribute significantly to the ring atmosphere.

Ring Characteristics

1. Cuzzi, J. et al. 1984. "Saturn's Rings: Properties and Processes," in Planetary Rings, edited by Greenberg and Brahic, 75-199. University of Arizona Press.

   This paper is an up-to-date summary of information on Saturn's rings. It contains a short section devoted

to the ring atmosphere, which concisely explains current knowledge on that subject. Also, a special interest is an appendix which outlines radiative transfer theory (which is so important in deducing ring characteristics from observations).

2. Esposito, L.W. et al. 1984. "Saturn's Rings: Structure, Dynamics and Particle Properties," in Saturn, edited by T. Gehrels and M. Matthews, 463-545. University of Arizona Press.

   This paper nicely complements the preceding paper (Cuzzi et al. 1984).

3. Marouf, E.A. et al. 1983. "Particle Size Distributions in Saturn's Rings from Voyager I Radio Occultation," Icarus 54: 189-211.

   This detailed paper provides the first precise estimates of particle size distributions ever given for the rings (results are calculated for four locations in the rings). The theory section in the paper also provides a clear application of radiative trasnfer theory.

4. Weidenschilling, S. et al. 1984. "Ring Particles: Collisional Interaction and Physical Nature," in Planetary Rings, edited by Greenberg and Brahic, 367-415. University of Arizona Press.

   Besides providing an in-depth analysis of the effect of collisions between ring particles on the evolution of the rings, this paper gives information useful in the study of particle properties.

Miscellaneous

1. Chandrasekhar, S. 1960. Radiative Transfer. Dover Publications, Inc.

   Chandrasekhar produced the definitive work in the field of radiative transfer (radiative transfer theory seeks to specify the radiation field produced when incident radiation is scattered and absorbed by media consisting of discrete particles). This book is rigorous in approach, in fact it can be appreciated as a work in mathematical physics, alone. It is not light reading.

2. Pollack, J.B. 1975. "The Rings of Saturn," Space Science Review 18: 3-93.

   Pollack's paper is a review of knowledge on Saturn's rings up to 1975. Much has been discovered since then,

AD-A171 687 THE ATMOSPHERE AROUND SATURN'S RINGS: A STUDY OF THE PROBABILITY OF COLLI (U) NAVAL POSTGRADUATE SCHOOL MONTEREY CA D F BEDEY JUN 86 2/2

UNCLASSIFIED F/G 3/2 NL

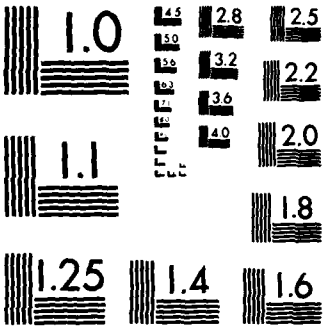

rendering invalid some of the predictions in the paper. This does not distract from the value of his work as a historical review. Reading this paper is an inspirational experience, because Pollack clearly demonstrates how knowledge about the rings increased through application of the scientific method.

3. van de Hulst, H.C. 1981. Light Scattering by Small Particles. Dover Publications, Inc.

This book is very readable. It essentially connects the mathematical physics of Chandrasekhar (1960) with the world of applied research. It provides the means by which the measurement of light scattering can be used to deduce the properties of the scattering medium.

LIST OF REFERENCES

Barker, E., et al., "Lyman-alpha Observations in the Vicinity of Saturn with Copernicus," Astrophysical Journal, v. 242, pp. 383-394, 1980.

Blamont, J., "The 'Atmosphere' of the Rings of Saturn," in The Rings of Saturn (NASA SP-343), edited by Palluconi and Pettengill, pp. 125-129, U.S. Government Printing Office, 1974.

Brackmann, R. and Fite, W., "Condensation of Atomic and Molecular Hydrogen at Low Temperatures," Journal of Physical Chemistry, v. 34, pp. 1572-1579, 1961.

Bridges, F., Hatzes, A., and Lin, D.N.C., "Structure, Stability and Evolution of Saturn's Rings," Nature, v. 309, pp. 333-335, 1984.

Broadfoot, A.L., et al., "Extreme Ultraviolet Observations from Voyager I Encounter with Saturn," Science, v. 212, pp. 206-211, 1981.

Carlson, R.W., "Photo-sputtering of Ice and Hydrogen around Saturn's Rings," Nature, v. 283, 1980.

Chandrasekhar, S., Radiative Transfer, Dover Publications, Inc., 1960.

Cheng, A.F. and Lanzerotti, L.J., "Ice Sputtering by Radiation Belt Protons and the Rings of Saturn and Uranus," Journal of Geophysical Research, v. 83, pp. 2597-2602, 1978.

Cheng, A.F., Lanzerotti, L.J., and Pirronello, V., "Charged Particle Sputtering of Ice Surfaces in Saturn's Magnetosphere," Journal of Geophysical Research, v. 87, pp. 4567-4570, 1982.

Clarke, J.T., et al., "IUE Detection of Bursts of H Lyα Emissions from Saturn," Nature, v. 290, pp. 226-227, 1981.

Cuzzi, J., et al., "Saturn's Rings: Properties and Processes," in Planetary Rings, edited by Greenberg and Brahic, pp. 73-199, University of Arizona Press, 1984.

Dennefeld, M., "Theoretical Studies of an Atmosphere around Saturn's Rings," in Exploration of the Planetary System, edited by Woszczyk and Iwaniszewska, pp. 471-481, Reidel, 1974.

Durisen, R.H., "Transport Effects due to Particle Erosion Mechanisms," in Planetary Rings, edited by Greenberg and Brahic, pp. 416-446, University of Arizona Press, 1984.

Esposito, L.W., et al., "Saturn's Rings: Structure, Dynamics and Particle Properties," in Planetary Rings, edited by Greenberg and Brahic, pp. 463-545, University of Arizona Press, 1984.

Ip, W.-H., "On the Lyman-alpha Emission from the Vicinity of Saturn's Rings," Astronomy and Astrophysics, v. 70, pp. 435-437, 1978.

Ip, W.-H., "Collisional Interaction of Ring Particles and the Ballistic Transport Process," Icarus, v. 54, pp. 253-262, 1983.

Judge, D.L. and Carlson, R.W., "Ultraviolet Photometer Observations of the Saturnian System," Science, v. 207, pp. 431-434, 1980.

Kerr, R.A., "Making Better Planetary Rings," Science, v. 229, pp. 1376-1377, 1985.

Marouf, E.A., et al., "Particle Size Distributions in Saturn's Rings from Voyager I Radio Occultation," Icarus, v. 54, pp. 189-211, 1983.

Morfill, G.E., et al., "Some Consequences of Meteroid Impacts on Saturn's Rings," Icarus, v. 55, pp. 439-447, 1983.

Null, G.W., et al., "Saturn Gravity Results Obtained from Pioneer II Tracking Data and Earth-based Saturn Satellite Date," Astronomical Journal, v. 86, pp. 456-468, 1981.

Shemansky, D.E. and Smith, G.R., "Whence Comes the 'Titan' Hydrogen Torus?," EOS, v. 63, p. 1019, 1982.

Tyler, G.L., et al., "The Microwave Opacity of Saturn's Rings at Wavelengths of 3.6 and 13 cm from Voyager I Radio Occultation," Icarus, v. 54, pp. 160-188, 1983.

van de Ulst, H.C., Light Scattering by Small Particles, Dover Publications, Inc., 1981.

Weidenschilling, S., et al., "Ring Particles: Collisional Interactions and Physical Nature," in Planetary Rings, edited by Greenberg and Brahic, pp. 367-415, University of Arizona Press 1984.

Weiser, H., Vitz, R.C., and Moos, H.W., "Detection of Lyman-α Emission from the Saturnian Disk and from the Ring System," Science, v. 197, pp. 755-756, 1977.

INITIAL DISTRIBUTION LIST

		No. Copies
1.	Defense Technical Information Center Cameron Station Alexandria, Virginia 22304-6145	2
2.	Library, Code 0142 Naval Postgraduate School Monterey, California 93943-5000	2
3.	Department Chairman, Code 61 Department of Physics Naval Postgraduate School Monterey, California 93943-5000	1
4.	Prof. R. Armstead, Code 61Ar Department of Physics Naval Postgraduate School Monterey, California 93943-5000	1
5.	Prof. K. Woehler, Code 61Wh Department of Physics Naval Postgraduate School Monterey, California 93943-5000	1
6.	CPT David F. Bedey Department of Physics United States Military Academy West Point, New York 10996	2

END

DTIC

10-86